6
THE GLOBAL IRON CYCLE

Brian Kendall[1], Ariel D. Anbar[1,2], Andreas Kappler[3] and Kurt O. Konhauser[4]

[1]School of Earth and Space Exploration, Arizona State University, Tempe, Arizona, 85287, USA
[2]Department of Chemistry and Biochemistry, Arizona State University, Tempe, Arizona, 85287, USA
[3]Geomicrobiology, Center for Applied Geosciences, University of Tübingen, Sigwartstrasse 10, 72076, Tübingen, Germany
[4]Department of Earth and Atmospheric Sciences, University of Alberta, Edmonton, Alberta, T6G 2E3, Canada

6.1 Overview

It should come as no surprise that iron, the fourth most abundant element in the Earth's crust (Taylor and McLennan, 1985), is essential in biology. Yet, in today's oceans, iron is a vanishingly rare element (Fig. 6.1). Its concentration – typically <1 nM (Johnson *et al*., 1997; Boye *et al*., 2001; Cullen *et al*., 2006) – is so low that iron scarcity limits biological productivity across large areas of the Earth's surface (Martin and Fitzwater, 1988). This peculiar situation is a consequence of the chemical behaviour of iron on an oxygenated Earth. In the presence of abundant O_2, the element is found primarily in the Fe(III) oxidation state, which forms poorly soluble oxyhydroxides. Why, then, is iron required by biology? Most likely, this is a legacy of early evolution when iron was ubiquitous on land and in the sea. It also helped that iron binds strongly to a variety of anionic ligands (involving oxygen, nitrogen, and sulfur) and could readily have been incorporated into biological compounds such as enzymes.

The story of iron geobiology is therefore a story in which the evolution of one geochemical cycle – that of oxygen – wreaked havoc with another – iron – that is essential to life's distribution on Earth. As O_2 levels rose, ocean iron abundances fell (Fig. 6.2). The acquisition of iron became more difficult. Microbes that depended on iron redox cycling for their metabolisms were driven from the ocean and land surface, which they once ruled, to the ocean depths. Eventually, they were confined to eking out a grubby living in ocean and lake sediments, where they dominate the biogeochemical cycling of iron to this day.

To understand this story and its implications, it is necessary to review the inorganic geochemistry of iron, its uses in biology, and the ways in which geochemistry and biology intersect in modern environments. These topics are addressed in Sections 6.2 and 6.3 below. In Section 6.4, we return to the evolutionary tale.

6.2 The inorganic geochemistry of iron: redox and reservoirs

Iron is the final product of nuclear fusion in stars because of its high binding energy per nucleon. It is therefore a relatively abundant element in the cosmos, and a major constituent of rocky planets. During early planetary differentiation, the high density of metallic iron relative to silicates caused iron to sink to the interior, so that it became the dominant constituent of the Earth's core. This is the Earth's major iron reservoir (Fig. 6.3). As a result of this partitioning, as well as later differentiation during partial melting of the mantle, the abundance of iron in the Earth's continental crust (~7 wt%; McLennan, 2001) is significantly less than in undifferentiated meteorites (~18 wt% in CI chondrites; Palme and Jones, 2003).

The redox state of the Earth's crust is such that iron in igneous crustal rocks occurs primarily in the Fe(II) oxidation state ('ferrous' iron), and also in the Fe(III) oxidation state ('ferric' iron), rather than as iron metal. Iron is present in igneous rocks in a wide range of minerals. It is a major constituent of common minerals such as the olivine mineral fayalite (Fe_2SiO_4), magnetite (Fe_3O_4) and pyrite (FeS_2), but is also found in a host of mineral classes such as pyroxenes, amphiboles and phyllosilicates.

Fundamentals of Geobiology, First Edition. Edited by Andrew H. Knoll, Donald E. Canfield and Kurt O. Konhauser.

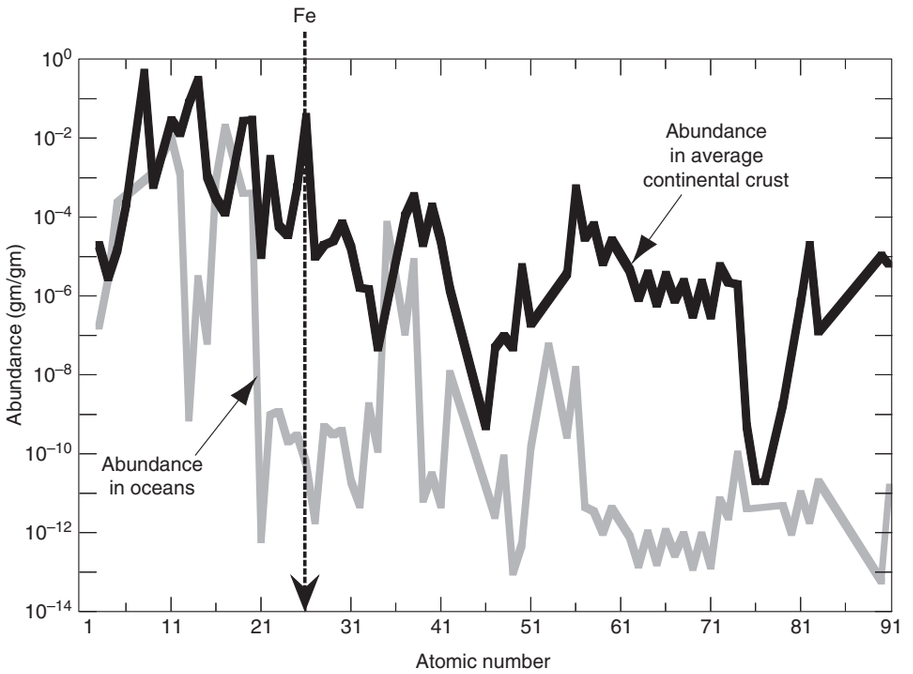

Figure 6.1 Abundance of the elements in the continental crust and oceans. Despite being one of the most abundant elements in the continental crust, iron has a very low concentration in the ocean.

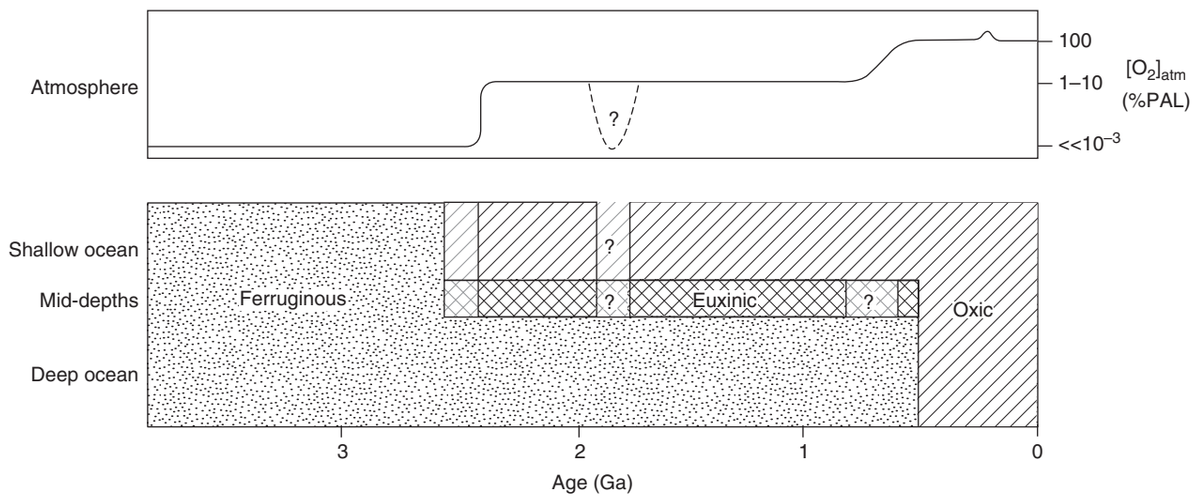

Figure 6.2 Redox conditions in the atmosphere and oceans over time. During the Archean when the atmosphere was essentially devoid of O_2, the oceans were predominantly anoxic and Fe(II)-rich (ferruginous) and sulfate-poor. Near the close of the Archean eon, the evolution of oxygenic photosynthesis led to limited O_2 accumulation along ocean margins. The first major increase in atmospheric O_2 at ~2.4 Ga was accompanied by widespread surface ocean oxygenation. Increased sulfate inputs to the oceans (from the oxidative weathering of crustal sulfide minerals) boosted rates of microbial hydrogen sulfide production along productive ocean margins (sites of high organic carbon export), leading to local expressions of anoxic and sulfidic (euxinic) conditions at mid-depths. The deep oceans remained ferruginous. This ocean redox structure likely held sway for the next ~2 Gyr, albeit with some spatiotemporal variation. Significant changes during this time include a possible decline in the atmosphere and ocean O_2 content at ~1.9 Ga, an expansion of euxinic and possibly low-O_2 conditions at 1.85 Ga that terminated the deposition of large iron formations, and a return to predominantly ferruginous oceans during the widespread, low-latitude Neoproterozoic glaciations. The onset of substantial deep-ocean oxygenation may have been delayed until the Ediacaran Period following a second major increase in atmospheric O_2 levels. Predominantly Oxygenated, iron-scarce oceans may not have been fully established until the Paleozoic. Modified from Lyons *et al*. (2009b).

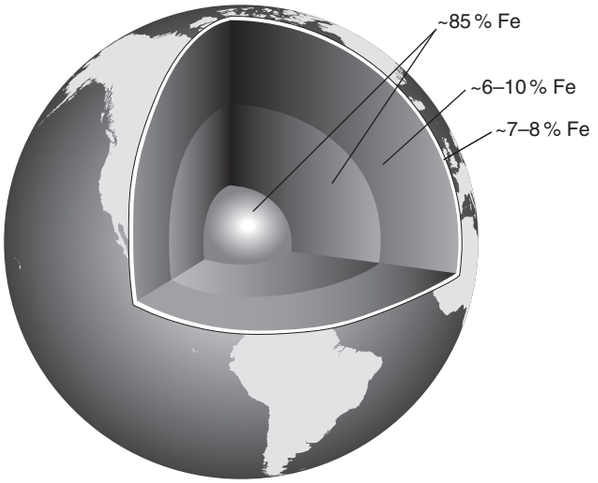

Figure 6.3 Iron distribution in the Earth. Most of the iron resides in the Earth's core as a result of early planetary differentiation that caused the dense iron metal to sink to the interior. Ocean crust (~8 wt%) is slightly enriched in iron relative to continental crust (~7 wt%). Classical estimates for the average mantle iron content were ~6 wt%. However, recent estimates suggest values closer to ~10 wt% for the lower mantle. Sources of data: crust – Hofmann (1988) and McLennan (2001); mantle – Palme and O'Neill (2003), Khan *et al*. (2008); Verhoeven *et al*. (2009) and Javoy *et al*. (2010); core – McDonough (2003) and Javoy *et al*. (2010).

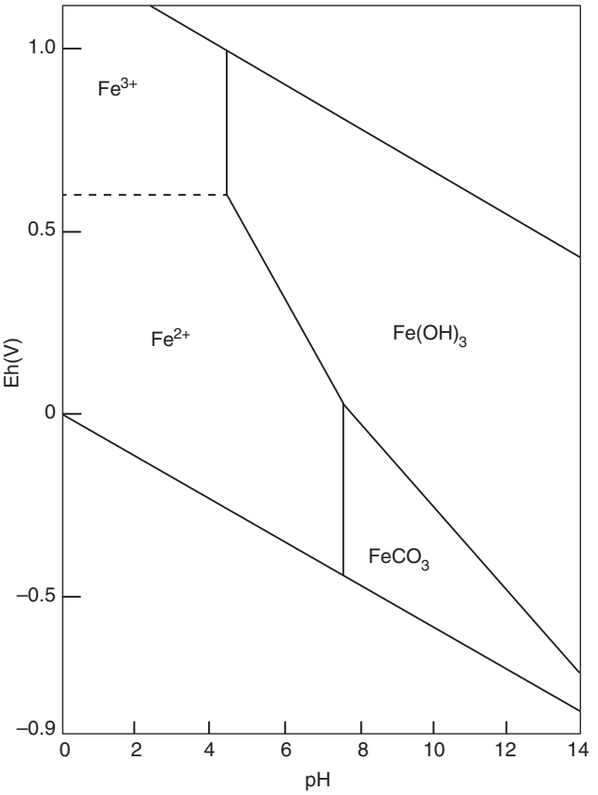

Figure 6.4 Eh-pH diagram for the Fe-O_2-H_2O-CO_2 system at 25 °C. The boundary between aqueous and solid phases is based on a dissolved iron concentration of 10^{-5} mol kg^{-1}. Modified from Langmuir (1997).

From a geobiological perspective, the iron cycle becomes interesting when chemical and biological weathering breaks down these iron-bearing minerals, releasing the element into aqueous solution. The transport and distribution of iron then depend strongly on pH, Eh (redox) and the presence or absence of other dissolved constituents that coordinate with Fe(II) or Fe(III) to form dissolved complexes, colloids or poorly soluble mineral phases. Biology strongly affects these parameters just as the availability of iron (or its absence) affects biological activity. These interactions give rise to complex and dynamic biogeochemical cycling of iron (Boyd and Ellwood, 2010; Konhauser *et al*., 2011a; Radic *et al*., 2011; Raiswell, 2011), as will be discussed in later sections.

The behaviour of iron is most strongly shaped by redox conditions because of the different chemical bonding affinities of Fe(II) and Fe(III). A chemical bond of particular importance to the transport and distribution of iron is that between Fe(III) and OH^- (the 'hydroxyl' ion). The equilibrium constant for the formation of $FeOH^{2+}$ is large ($K \approx 10^2$; Millero and Hawke, 1992; Millero *et al*., 1995; Stefánsson, 2007). The addition of further OH^- groups to Fe(III) is even more strongly favoured, leading to the formation of a host of neutral hydrolysis species such as FeOOH and $Fe(OH)_3$, and other hydrated Fe(III) oxyhydroxides such as disordered ferrihydrite ($Fe_{8.2}O_{8.5}[OH]_{7.4} + 3H_2O$), which ages to ferrihydrite ($5Fe_2O_3 \bullet 9H_2O$) (Michel *et al*., 2010). These species are only sparingly soluble, causing Fe to be removed from solution. Hence, the amount of iron dissolved in groundwaters, rivers and seawater decreases sharply with increasing Eh and pH (Fig. 6.4).

Iron can also be effectively removed from solution under the opposite condition of low Eh if there is an abundance of dissolved sulfide (HS^- and H_2S). Under these conditions, Fe(II) reacts readily to form mono- and disulfide species, leading ultimately to the production of insoluble iron sulfide (pyrite) via a series of intermediate iron–sulfur species (Luther, 1991; Schoonen and Barnes, 1991). This is a major pathway for the immobilization of iron in anoxic environments, such as in sulfide-rich lakes and ocean basins, and the pore fluids of marine sediments and soils (Berner, 1970, 1984). This chemistry couples the biogeochemistry of iron to that of sulfur. When Fe(II) is in excess of HS^-, iron can be removed from solution in the presence of bicarbonate and phosphate, leading to the formation of siderite and vivianite, respectively (Krom and Berner, 1980; Coleman, 1985).

A major consequence of these chemical characteristics is that iron is typically scarce in modern natural waters, at least in comparison to its abundance in rocks. During oxidative weathering, Fe(III) is produced and immediately immobilized, generating iron oxide residues and leaving average river water with a typical dissolved iron concentration of only ~40 nM (higher concentrations can be found in rivers draining peatlands); a large fraction of the iron load in rivers is colloidal or suspended (Dai and Martin, 1995; Krachler *et al*., 2005, 2010). Colloidal iron is largely removed from solution during mixing of freshwaters with seawater in estuaries. There, the high ionic strength of seawater neutralizes surface charges on colloidal particles, allowing them to coagulate and precipitate (Gustafsson *et al*., 2000; Krachler *et al*., 2010). Far from shore, then, other sources may be more important (Fig. 6.5). Most notable are dust particles, which are believed to be the primary source of iron to the open oceans (Jickells *et al*., 2005). In glaciated regions, the flux of bioavailable iron supplied by melting glaciers and icebergs can be similar to the aeolian flux, as shown for the Southern Ocean (Lannuzel *et al*., 2008; Raiswell *et al*., 2008). However, as on land, chemical decomposition of these particles rapidly results in the production of ferric oxyhydroxide particulates. A major challenge for marine ecosystems, then, is to acquire this iron before particulates settle to the seafloor. In general, the transport of iron from the continents to the open ocean is thought to be dominated by the formation of nanoparticulate oxyhydroxides. Stabilization ('ageing') of these nanoparticles is suggested to permit long-distance transport to sites in the open ocean where they can be converted ('rejuvenated') to more bioavailable forms (Raiswell, 2011).

Iron derived from high-temperature hydrothermal systems in the deep sea may constitute another source (Chu *et al*., 2006; Bennett *et al*., 2008). It was thought that most of this iron is removed either as pyrite in sulfide-rich vent fluids or as ferrihydrite when hydrothermal plumes mix with oxygenated seawater (Lilley *et al*., 2004). However, recent spectromicroscopic measurements of carbon and iron in particles from hydrothermal plumes on the East Pacific Rise suggests that some Fe(II) is stabilized by organic complexation, preventing its removal into insoluble minerals. Such particles may then provide a source of bioavailable iron to environments outside of the mid-ocean ridge (Toner *et al*., 2009). In oxygen-deficient Precambrian oceans, hydrothermal sources were probably an important source of iron to seawater, and enabled the formation of massive deposits of chemical sediment known as iron formation (see Chapter 8).

An additional, but poorly quantified, source of ferrous iron is dissolved in sedimentary pore fluids that are anoxic, or nearly so, but not sulfidic. Such pore fluids occur on continental margins, where high biological productivity in overlying seawater yields a high flux of organic carbon to the sediments on continental shelves. This influx of reduced carbon generates anoxia, allows microbial Fe(III) reduction to take place, and hence results in the presence of dissolved Fe(II), the concentration of which may approach ppm levels in pore fluids. Benthic iron fluxes from river-dominated continental margins could potentially be orders of magnitude greater than non-river dominated shelves. Some of this iron may escape to seawater and hence provide a critical source of iron to near-shore ecosystems (Severmann *et al*., 2010). This process is also known to occur on the

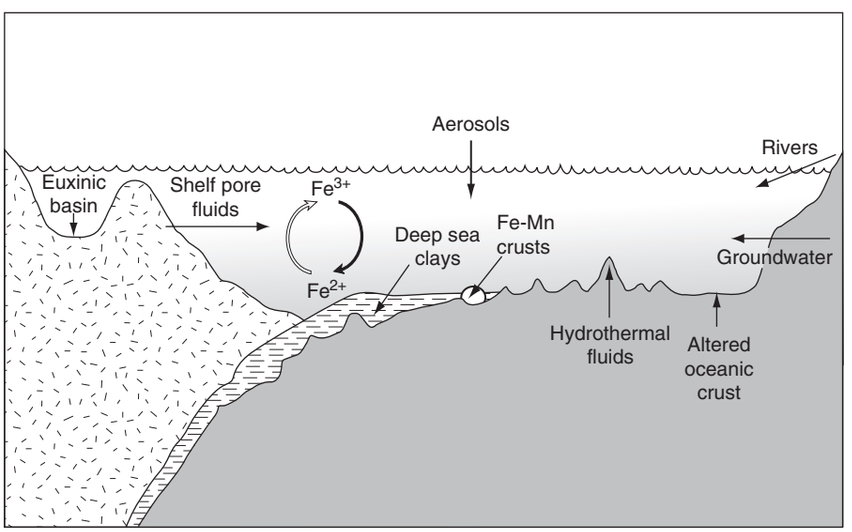

Figure 6.5 Schematic diagram illustrating the sources and sinks of iron in modern seawater. Dissolved and particulate iron is supplied to seawater by rivers, groundwaters, aeolian dust, hydrothermal vents and alteration of oceanic crust, and anoxic pore waters along continental margins. In glaciated regions, iron would also be supplied by melting glaciers and icebergs. In oxygenated seawater, iron is oxidized and precipitated as poorly soluble iron oxyhydroxides that are removed into sediments. Iron is also removed as insoluble iron sulfide minerals in restricted euxinic basins such as the Black Sea. Modified from Anbar and Rouxel (2007).

shelves of basins containing anoxic and sulfidic deep waters, such as the Black Sea. Systematic studies of sedimentary iron speciation and iron isotopes in such basins demonstrate that pore fluid-derived iron migrates along the chemocline to the deep basins, where it is immobilized as pyrite (Lyons and Severmann, 2006; Severmann *et al*., 2008; Fehr *et al*., 2010).

Unsurprisingly in view of these considerations, iron has a very short residence time of only up to a few hundred years in the modern oceans (Johnson *et al*., 1997). As a result, iron is ubiquitous in marine sediments. Outside of sulfidic basins, it is delivered to the seafloor as ferric oxyhydroxide precipitates. However, as these precipitates are buried, bacterial sulfate reduction generates H_2S or HS^- (depending on pore fluid pH) in sedimentary pore fluids, converting a large fraction of these ferric oxides to ferrous sulfides.

6.3 Iron in modern biology and biogeochemical cycles

6.3.1 Fe as a micronutrient

Iron is essential to most organisms. It is generally found in the centre of metalloproteins that mediate redox reactions. Some of these proteins serve as enzymes that facilitate the transfer of electrons used to generate chemical energy for the cell. Some major Fe-containing enzymes include hydrogenases, iron–sulfur proteins and cytochromes. Hydrogenases are proteins that catalyse the reduction of a substrate by adding H_2, which can be obtained from either various intracellular respiratory processes, or extracellularly from aqueous solution. Iron–sulphur proteins are electron carriers that range from simple molecules containing one Fe–S centre to complexes containing multiple types of Fe–S clusters. Fe_2S_2 (ferredoxin) and Fe_4S_4 are the most common. Each Fe–S centre has at least two redox states, a reduced ferrous form and an oxidized ferric form, and each centre carries only one electron at a time. Cytochromes are proteins that have an iron-containing porphyrin ring (known as heme) that is capable of alternating between Fe(II) and Fe(III). There are a number of different cytochromes based on differences in the side groups of the porphyrin ring (heme *a*, *O*, *b*, *c* and *d*), each with a different electrode potential, and hence each occurs in a different location in the electron transport chain. Some serve as the terminal reductases in metabolic pathways, passing the electrons onto a terminal electron acceptor, whereas other cytochromes specifically facilitate the transfer of electrons from the external environment into the transport chain (i.e. those that oxidize Fe(II), H_2, H_2S, and $S_2O_3^{2-}$).

Other Fe-containing enzymes (nitrogenase) are found in organisms that fix atmospheric nitrogen gas (N_2). Nitrogenase catalyses the breaking of the triple bonds between each nitrogen atom, and then bonds the nitrogen to hydrogen atoms via the reaction: $N_2 + 3H_2 \rightarrow 2NH_3$. All nitrogenases have an iron- and sulfur-containing cofactor that facilitates the electron transfers. Due to the oxidative properties of O_2 on the Fe–S cofactors, most nitrogenases are irreversibly inhibited by the presence of O_2. Thus, nitrogen fixing organisms utilize mechanisms to exclude O_2 – a particular challenge for cyanobacteria that produce O_2 via photosynthesis. Some cyanobacteria cope by expressing specialized non-photosynthetic cells within their filaments (called *heterocysts*) that serve as O_2-free microenvironments for nitrogen fixation (Fay *et al*., 1968). Other cyanobacteria photosynthesize strictly during daylight and fix nitrogen at night (Bebout *et al*., 1993).

6.3.2 Fe in redox reactions

6.3.2.1 Aerobic Fe(II) oxidation

The occurrence of bacteria that gain energy from the oxidation of Fe(II) to Fe(III) is generally limited by the availability of dissolved Fe^{2+}. This is not an insignificant problem because at neutral pH and under fully aerated conditions, Fe(II) rapidly oxidizes chemically to Fe(III), which is then hydrolysed to ferrihydrite. The kinetic relationship that describes chemical Fe(II) oxidation at circumneutral pH values is:

$$\frac{\mathrm{d[Fe(II)]}}{\mathrm{d}t} = k[\mathrm{Fe(II)}][\mathrm{OH}^-]p\mathrm{O}_2$$

where $k = 8(\pm 2.5) \times 10^{13}$ $\mathrm{min^{-1}\ atm^{-1}\ mol^{-2}\ l^{-2}}$ at 25 °C (Singer and Stumm, 1970). As is evident from the equation, pH and oxygen availability have strong influences on the reaction rate, which explains why at low pH or low oxygen concentrations, dissolved Fe^{2+} is quite stable (e.g. Liang *et al*., 1993). Accordingly, the most efficient way for a microorganism to survive on Fe(II) is to either grow under acidic conditions (as an acidophile) or under low-O_2 conditions at circumneutral pH (as a microaerophile) because in both cases, the chemical reaction kinetics are sufficiently diminished that microorganisms can harness Fe(II) oxidation for growth.

There are a number of acidophilic Fe(II)-oxidizing bacteria that grow autotrophically on Fe(II), using O_2 as its terminal electron acceptor (Blake and Johnson, 2000):

$$2Fe^{2+} + 0.5O_2 + 2H^+ \rightarrow 2Fe^{3+} + H_2O$$

The best characterized acidophiles are *Acidothiobacillus ferrooxidans* and *Leptospirillum ferrooxidans*. They grow well at mine waste disposal sites where reduced sources of iron are continuously regenerated during acid mine drainage. Another iron-oxidizing bacterium is *Sulfolobus*

acidocaldarius that lives in hot, acidic springs at temperatures near boiling. All of the Fe(II)-oxidizing bacteria use ferrous iron for both the generation of energy (in the form of ATP [adenosine triphosphate]) and reducing power to convert CO_2 into organic carbon. Since it takes on average 50 mol of Fe^{2+} to assimilate 1 mol of carbon (Silverman and Lundgren, 1959), cells such as *A. ferrooxidans* must oxidize a large amount of ferrous iron in order to grow. Consequently, even a small number of bacteria can be responsible for generating significant concentrations of Fe^{3+}.

Under neutral pH, but with O_2 levels below 1.0 mg l^{-1} and redox conditions about 200–300 mV lower than typical surface waters (characteristics of some iron-rich springs, stratified bodies of water and hydrothermal vent systems), microaerophilic bacteria, such as *Gallionella ferruginea*, play an important role in Fe(II) oxidation. *Gallionella*-type oxidizers are bean-shaped cells that grow at the terminus of a helical structure called a stalk which is composed largely of polysaccharides frequently encrusted by ferrihydrite (Hanert, 1992). Unlike the acidophiles, the neutrophiles can harness much more energy because at pH 7, the electrode potential of the couple $Fe(OH)_3/Fe^{2+}$ ($E^{0'} \approx 0$ V; Thamdrup, 2000) is substantially lower than the redox couple of O_2/H_2O ($E^{0'} = 0.81$ V). This indicates that Fe(II) oxidation can generate significant energy at circumneutral pH to support ATP production. Although *G. ferruginea* grows chemotrophically at a pH just below 7 on a medium with Fe(II) salts and fixes all of its carbon autotrophically from CO_2 (Hallbeck and Pedersen, 1991), there is at present no conclusive evidence that they actually derive energy from Fe(II) oxidation. Interestingly, *G. ferruginea* does not form a stalk at a pH < 6 or under very micro-oxic conditions, where O_2 is present but the redox potential is −40 mV (Hallbeck and Pederson, 1990). This suggests that the stalk represents an organic surface upon which ferrihydrite can precipitate and, in doing so, protect the cell itself from becoming mineralized. In a similar manner, it has been suggested that another bacterium, *Leptothrix ochracea*, induces ferrihydrite precipitation on its sheath as a means to detoxify the presence of any free oxygen in their environment (Nealson, 1982). These examples certainly imply that Fe(II) oxidation need not be directly tied to energy production.

6.3.2.2 Anaerobic chemolithoautotrophic Fe(II) oxidation

Ferrous iron has also been observed to undergo microbial oxidation under anoxic conditions thus closing the iron redox cycle even in O_2-free environmental systems (Fig. 6.6). In anoxic environments, Fe(II) is relatively stable since neither nitrate nor sulfate react chemically with Fe(II) at appreciable rates at low temperature. Only Mn(IV) and high concentrations of nitrite have been shown to be relevant abiotic chemical oxidants for Fe(II) (Buresh and Moraghan 1976; Rakshit *et al*. 2008). Biological oxidation of Fe^{2+} in the absence of oxygen can occur via photoferrotrophy (discussed below) and chemoautotrophy. During the latter process, oxidation of Fe^{2+} occurs in the absence of light with nitrate as the electron acceptor according to the following equation (Straub *et al*., 1996):

$$10Fe^{2+} + 2NO_3^- + 24H_2O \rightarrow 10\ Fe(OH)_3 + N_2 + 18H^+$$

Nitrate-dependent Fe(II) oxidation has been shown to be widespread in sediments (Straub and Buchholz-Cleven, 1998). Most of the described nitrate-reducing, Fe(II)-oxidizing strains depend on an organic

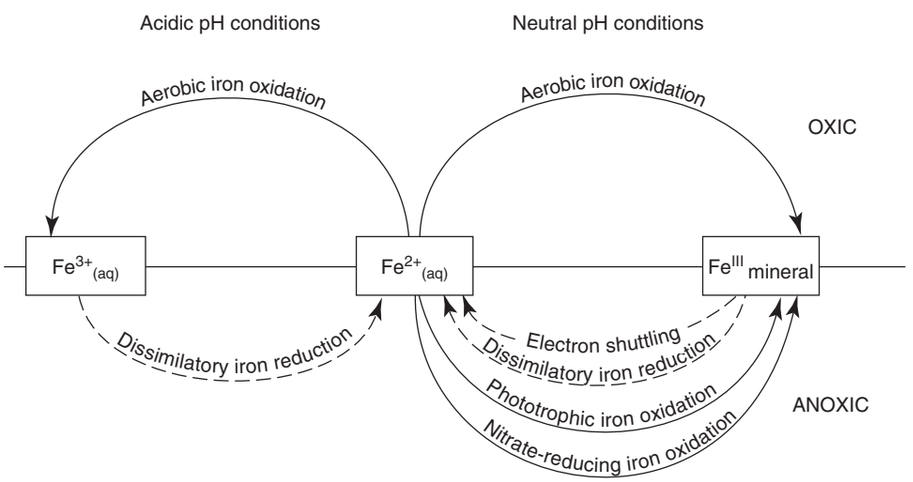

Figure 6.6 Schematic diagram summarizing the microbial iron redox reactions under conditions of acidic and neutral pH.

co-substrate (e.g. acetate, Kappler *et al*., 2005a) and truly lithoautotrophic strains have not been isolated in pure culture. Weber *et al*. (2006) isolated an Fe(II)-oxidizing bacterium that was suggested to be able to oxidize Fe(II) autotrophically; however, this strain could not be transferred continuously in lithoautotrophic culture. Similarly, some strains of nitrate-dependent bacteria oxidizing Fe(II) in the absence of an organic co-substrate were isolated from the deep oceans (Edwards *et al*., 2003), but it is unclear whether these strains can be cultivated for successive generations with Fe(II) as the sole electron donor. So far, the chemolithoautotrophic enrichment culture described by Straub *et al*. (1996) is the only culture oxidizing Fe(II) with nitrate autotrophically (without the addition of any organic substrate). From gene analysis it is known that this culture consists of four organisms, including three chemoheterotrophic nitrate-reducing bacteria (*Parvibaculum lavamentivorans*, *Rhodanobacter thiooxidans* and *Comamonas badia*), plus a fourth organism related to the chemolithoautotrophic Fe(II)-oxidizing bacterium *Sideroxydans lithotrophicus* (Blothe and Roden, 2009). The complexity of this culture potentially suggests that a consortium of organisms is needed for autotrophic Fe(II) oxidation coupled to nitrate-reduction.

In contrast to the microaerophilic strains discussed above, at least one mixotrophic nitrate-reducing Fe(II)-oxidizing strain (*Acidovorax* sp. BoFeN1) was shown to benefit directly from Fe(II) oxidation. Higher cell numbers were observed when oxidizing Fe^{2+} and the organic co-substrate compared to oxidation of the organic compounds alone (Muehe *et al*., 2009). During Fe(II) oxidation, these organisms precipitate goethite, lepidocrocite, ferrihydrite or poorly crystalline Fe(III) phosphates depending on the geochemical conditions (Miot *et al*., 2009; Larese-Casanova *et al*., 2010). They precipitate iron minerals distant to the cells but also form mineral crusts at the cell surface and in the space between the outer and inner cell membranes, known as the periplasm (Miot *et al*., 2009). These electron microscopical and synchrotron-based spectro-microscopical studies, in combination with iron isotope analysis (Kappler *et al*., 2010), suggest that Fe(II) oxidation takes place at least to some extent in the periplasm.

6.3.2.3 Photosynthetic Fe(II) oxidation

The existence of anoxygenic photosynthetic Fe(II) oxidation (photoferrotrophy) was suggested nearly 20 years before the discovery of the first microorganisms catalysing this reaction. Garrels *et al*. (1973) and Hartmann (1984) suggested photoferrotrophy as a deposition mechanism for iron formation under O_2-free conditions in the Precambrian. Light instead of O_2 could have facilitated Fe(II) oxidation, via photosynthesis that used Fe(II) rather than H_2O as an electron donor, producing Fe(III) instead of O_2. Two decades later this hypothesis was validated by the discovery of the first photoferrotrophic microorganisms (Widdel *et al*., 1993). Currently, a variety of phylogenetically diverse strains of anoxygenic Fe(II)-oxidizing phototrophs including purple sulfur, purple non-sulfur, and green sulfur bacteria are known to catalyse oxidation of Fe(II) to Fe(III) according to the following reaction (Hegler *et al*., 2008):

$$4\,Fe^{2+} + HCO_3^- + 10H_2O + h\nu \rightarrow 4\,Fe(OH)_3 + (CH_2O) + 7H^+$$

where $h\nu$ is a quantum of light.

Both the aerobic and anaerobic Fe(II)-oxidizing bacteria face the problem of limited availability of dissolved Fe(II) and the possible inhibitory effect of the very poor solubility of the ferric oxyhydroxide end products of their metabolism. The formed particles are positively charged due to their high points of net zero charge (ZPC); e.g. pH ≈ 8 for ferrihydrite (Posth *et al*., 2010). Therefore, in the proximity of cells, Fe(III) cations, colloids and particles are expected to adsorb to cell surfaces that are in general negatively charged due to a high content of carboxylic, phosphoryl and/or hydroxyl groups. On the one hand, Fe(III) encrustation can lead to the accumulation of trace metals and nutrients that naturally adsorb onto such particles. Other advantages include protection from dehydration, while the protons released during Fe(III) mineral precipitation near the cell surface could also increase the energy yield of iron oxidation by increasing the pH-gradient utilized in the proton motive force (Chan *et al*., 2004). The downside of iron encrustation comes from the potential reduction in the diffusion and uptake of substrates and nutrients to the cell, leading to the stagnation of cell metabolism and eventually to cell death. In terms of light availability, iron encrustation can have opposing effects; it may limit absorption of key wavelengths of light, but the minerals may serve as a UV-shield to protect against damage by high radiation (Phoenix *et al*., 2001).

For the stalk- or sheath-forming aerobic Fe(II)-oxidizing bacterial genera *Gallionella* and *Leptothrix*, it was suggested that the microbially produced and excreted organic matrices are used for extracellular capture of the Fe(III) minerals produced. However, for these strains it remains unanswered where the Fe(II) is oxidized (i.e. in the cytoplasm, in the periplasm, or at the cell surface). In terms of the photoferrotrophs, it has recently been proposed that Fe(II) oxidation happens in the periplasm of the cells (Croal *et al*., 2004; Jiao and Newman, 2007). Since cell encrustation is not observed this further raises the question of how Fe(III) is transported out of the cytoplasm to the cell exterior and then away from the

cells without sorbing to the organic ligands. An acidic pH microenvironment, the use of organic ligands to keep the Fe(III) in solution in close proximity to the cell, or the shedding off of organic-mineral aggregates from the cell surface have all been suggested as plausible methods used by the bacteria (Kappler and Newman 2004; Schädler *et al*., 2009; Hegler *et al*., 2010).

6.3.2.4 Anaerobic Fe(III) reduction

In addition to primary producers, there are a variety of other species that heterotrophically break down existing organic carbon to either carbon dioxide or methane gas. The type of heterotrophic metabolism that occurs in nature depends on what oxidants are available and, in the situation when multiple electron acceptors are present (as in the uppermost sediment layers), on the free energy yield of the specific reaction. Thus, the decomposition of freshly deposited organic material in sediments proceeds in a continuous sequence of redox reactions, with the most electropositive oxidants (such as O_2 and $NO_3^-)^-$ consumed at or near the surface, and progressively poorer oxidants (Mn(IV), Fe(III), SO_4^{2-}, and CO_2) consumed at depth until the labile organic fraction is exhausted and the deeper sediments are left with a composition very different from the sediments originally deposited (Froehlich *et al*., 1979).

Below the zone of dissimilatory Mn(IV) reduction, and at the depth of complete nitrate removal from pore waters, is where Fe(III) reduction takes place. Dissimilatory iron reduction is broadly distributed amongst several known bacterial genera. *G. metallireducens* and *S. putrefaciens* were among the first bacteria studied in pure culture that could gain energy from coupling Fe(III) reduction to the oxidation of H_2 and/or simple fermentation products, including short- and long-chain fatty acids, alcohols and various monoaromatic compounds:

$$CH_3COO^- + 8Fe(OH)_3 \rightarrow 8Fe^{2+} + 2HCO_3^- + 15OH^- + 5H_2O$$

Since then, many more species, including a number of hyperthermophilic Archaea, some sulfate- and nitrate-reducers, and methanogens have shown the capacity for reducing ferric iron minerals (Lovley *et al*., 2004).

Ferric iron minerals occur in soils and sediment in a wide variety of forms, ranging from amorphous to crystalline phases. The amorphous to poorly-ordered iron oxyhydroxides, such as ferrihydrite or goethite, are the preferred sources of solid-phase ferric iron for Fe(III)-reducing bacteria (Lovely and Phillips, 1987). More crystalline Fe(III) oxides (e.g. hematite and magnetite) and Fe-rich clays (e.g. smectite) are also microbially reducible, and some experimental observations suggest that these minerals may provide energy for cellular growth comparable to that derived from the poorly crystalline phases (e.g. Roden and Zachara, 1996; Kostka *et al*., 2002), although this may only be the case for optimal experimental conditions. Variations in Fe(III) reduction rates are related to a number of factors, including the amount of surface area exposure, crystal morphology, particle aggregation, composition of the aqueous solution in which the microorganisms grow, and the amount of Fe^{2+} sorbed to the oxide surface (e.g. Urrutia *et al*., 1998). Importantly, with such great heterogeneity in reactivity towards microbial reduction, it is not surprising that Fe(III) can represent a long-term electron acceptor for organic matter oxidation, even at sediment depths where other anaerobic respiratory processes are thermodynamically predicted to dominate (Roden, 2003).

Until recently, it was believed that the reduction of ferric iron-containing minerals (dissolved Fe^{3+} dominates at pH < 4) necessitated direct contact of the microorganism with the mineral surface. Once in contact with the surface, the Fe(III)-reducers are faced with the problem of how to effectively access an electron acceptor that cannot diffuse into the cell. These criteria thus require that Fe(III)-reducing bacteria must not only be able to actively recognize an iron mineral surface and attach to it, but that they must also be capable of activating or producing proteins that specifically interact with that mineral surface. Work with species such as *G. metallireducens* has shown that they are chemotactic and are able to sense the gradient of reduced metal ions emanating from the dissolution of the oxyhydroxide phases under anoxic conditions. After moving towards the solid phases, the bacteria specifically express flagella and pili that help them adhere to the Fe(III) oxyhydroxides (Childers *et al*., 2002). Alternatively, *Shewanella algae* relies on the production of hydrophobic surface proteins that facilitate greater cell adhesion (Caccavo *et al*., 1997). Once the bacteria attach to the mineral surface they begin shuttling electrons from a reduced source within the cytoplasm, across the plasma membrane and periplasmic space, to the outer membrane. Located there are iron reductase enzymes that transfer those electrons directly to the Fe(III) mineral surface, causing a weakness in the Fe–O bond and invariably its reductive dissolution (Lower *et al*., 2001). Electron transfer via direct contact between cells and the mineral surface has been suggested to be mediated also via conductive pili (Reguera *et al*., 2005; Gorby *et al*., 2006; El-Naggar *et al*., 2010).

More recently, it was discovered that other Fe(III)-reducing bacteria, such as *Shewanella* species, overcome the solubility problem by utilizing dissolved or even non-dissolved organic compounds as electron shuttles between the cell surface and the Fe(III) oxides, which may be located at some distance away from the cell. One example is the quinone moieties in exogenous humic

compounds which bacteria can reduce to the semiquinone and hydroquinone oxidation state via the oxidation of acetate or lactate (Lovley *et al*., 1996; Jiang and Kappler, 2008; Roden *et al*., 2010). The reduced humics subsequently transfer electrons abiotically to Fe(III), producing Fe^{2+}, and in doing so, regenerate the oxidized form of the humic compound for another cycle. The extent of electron transfer from reduced humics to Fe(III) was shown to depend on the redox potential of the Fe(III) species and thus on the type of Fe(III) minerals present (Bauer and Kappler, 2009). Some *Shewanella* species (*S. oneidensis*) have also been shown to produce and excrete their own quinone compounds that function in a similar manner to natural humics (Marsili *et al*. 2008; von Canstein *et al*., 2008), while the closely related *S. algae* produces soluble melanin which might serve as another type of electron conduit for Fe(III) oxyhydroxide reduction (Turick *et al*., 2002). Significantly, Fe(III) reduction rates are faster in the presence of organic electron shuttles than in their absence because they are likely to be more accessible for microbial reduction than poorly soluble Fe(III) oxyhydroxides (Nevin and Lovley, 2000).

6.3.3 Fe acquisition by siderophores

The poor solubility of Fe(III) at circumneutral pH and its correspondingly low concentrations in solution (~10^{-10} mol l^{-1}) means that it is often the limiting nutrient for growth. Many bacteria and fungi get around this impasse by excreting low molecular weight, Fe(III)-specific ligands known as siderophores (Neilands, 1989). In soils and seawater, siderophores or their breakdown products can be so abundant that they dominate ferric iron (e.g. Wilhelm and Trick, 1994). Siderophores have several properties that make them ideal Fe(III) chelators. They contain a general preponderance of oxygen atoms, are soluble, and provide bi- and multidente ligands that can form multiple coordinative positions around the central Fe^{3+} cation. Significantly, they form especially strong 1:1 surface complexes, and their association constants for Fe(III) can be several times higher than common soil organic acids (e.g. oxalic acid). This is an important property because it maintains dissolved iron in a soluble form that minimizes its loss from the aqueous environment by the precipitation of solid-phase ferric hydroxide (Hider, 1984).

The biosynthesis of siderophores is tightly controlled by iron levels. When soluble Fe^{3+} concentrations are low, siderophore production becomes activated by the presence of ferric iron-containing minerals, with higher levels of siderophores produced in response to increasingly insoluble iron sources (e.g. Hersman *et al*., 2000). Other studies have documented that some species generate different types and amounts of siderophores depending on the type of iron mineral present. Importantly, it appears that different siderophores are required to sequester Fe(III) from different iron minerals, and that changing the iron mineralogy can elicit a specific response from the same microorganism. In any event siderophores represent an extremely successful solution to the problem of obtaining dissolved iron from stable iron solid phases.

On a much larger scale, recent iron enrichment experiments in the equatorial Pacific have demonstrated that with the addition of soluble iron, a threefold increase in the concentration of Fe-binding organic ligands occurred, leading to a concomitant increase in microbial biomass production (Hutchins and Bruland, 1998). Interestingly, many species produce siderophores in great excess of their requirements (because many are lost via diffusion and advection), yet when levels of iron become sufficiently high (i.e. an order of magnitude above micromolar levels), their production is repressed and the cells meet their iron needs via low-affinity iron uptake systems (Page, 1993).

6.4 Iron through time

6.4.1 Evidence for major changes in biogeochemical cycles

6.4.4.1 Introduction

Iron is a redox-sensitive element. It forms poorly soluble iron oxyhydroxides in the presence of O_2, poorly soluble iron sulfides in the presence of dissolved sulfide, but soluble Fe(II) complexes in anoxic and sulfide-free environments. Hence, the biogeochemistry of iron, along with that of carbon and sulfur, is linked to the history of Earth surface oxygenation (Canfield, 2005; Lyons *et al*., 2009a; Poulton and Canfield, 2011). Ideally, the evolution of the iron biogeochemical cycle can be reconstructed from changes in the iron concentration of the oceans over geological time. Unfortunately, the rock record does not directly preserve samples of ancient seawater. Instead, we must infer the major changes in iron biogeochemical cycling through the petrological and geochemical characteristics of ancient sedimentary rocks such as iron formations (e.g. Konhauser *et al*., 2009; Bekker *et al*., 2010; Planavsky *et al*., 2010a) and fine-grained mudrocks (e.g. Canfield *et al*., 2008; Scott *et al*., 2008; Poulton *et al*., 2010; Planavsky *et al*., 2011). Even then, an additional complication arises from the fact that we cannot sample most of the sedimentary rocks deposited from pre-Jurassic open ocean seafloor because this material has since been recycled into the mantle by subduction at convergent plate margins. We have little choice but to rely upon the fragmentary sedimentary rock record, preserved along continental margins and in intracratonic basins, to draw our inferences on the evolution of the iron biogeochemical cycle.

In addition to episodes of iron formation deposition, a sizable fraction of our evidence for the spatiotemporal distribution of Fe(II) in the oceans comes from sedimentary iron speciation analyses of fine-grained sedimentary rocks. Briefly, as reviewed in Lyons and Severmann (2006), three basic parameters are employed: (1) the ratio of total iron to aluminum (Fe_T/Al), (2) the ratio of highly reactive iron to total iron (Fe_{HR}/Fe_T), and (3) the ratio of pyrite iron to highly reactive iron (Fe_{PY}/Fe_{HR}) (an older related term, the degree of pyritization [DOP], is a more conservative estimate of the degree to which Fe_{HR} has been converted to pyrite). As its name implies, Fe_{HR} comprises biogeochemically reactive iron, specifically pyrite plus other iron minerals (e.g. ferric oxides, magnetite, and iron-rich carbonates) that can react with sulfide in the water column or in sediments during early diagenesis (Poulton *et al*., 2004). Modern sediments deposited from locally anoxic bottom waters have ratios of Fe_{HR}/Fe_T that are higher (typically >0.38) compared to modern sediments deposited from oxygenated bottom waters (average = 0.26 ± 0.08; Raiswell and Canfield, 1998) and Phanerozoic oxic sediments (average = 0.14 ± 0.08; Poulton and Raiswell, 2002). Elevated ratios of Fe_{HR}/Fe_T (and Fe_T/Al) reflect Fe_{HR} transport, scavenging, and enrichment in sediments relative to background siliciclastic sources either because of pyrite formation in an anoxic and sulfidic (euxinic) water column or because of iron-rich mineral formation in an anoxic and Fe(II)-rich (ferruginous) water column (Poulton *et al*., 2004; Lyons and Severmann, 2006). The extent to which Fe_{HR} has been converted to pyrite is then used to determine whether the local water column was euxinic ($Fe_{PY}/Fe_{HR} > 0.8$) or ferruginous ($Fe_{PY}/Fe_{HR} < 0.8$) (Poulton *et al*., 2004).

6.4.4.2 Iron reigns supreme: the Archean oceans

Several lines of evidence point to an anoxic Archean atmosphere, including the preservation of mass-independent fractionation (MIF) of sulfur isotopes in sedimentary rocks ($pO_2 < 0.001\%$ of present atmospheric levels [PAL]; Farquhar *et al*., 2000, 2007; Pavlov and Kasting, 2002; Farquhar and Wing, 2003), the presence of detrital uraninite, pyrite and siderite in fluvial deposits (Fleet, 1998; Rasmussen and Buick, 1999; England *et al*., 2002; Hofmann *et al*., 2009), low Fe^{3+} to Fe_T ratios of spinels in Archean impact-produced spherules (Krull-Davatzes *et al*., 2010), and evidence for substantial iron mobilization and loss from paleosols during weathering (Rye and Holland, 1998; Sugimori *et al*., 2009). The Archean oceans were probably also anoxic and contained abundant iron in the form of dissolved Fe(II) complexes. The most obvious evidence for this are the iron formations – the major source of industrial iron ore (Fig. 6.7). A uniquely Precambrian rock type, many of these chemical sedimentary rocks comprise alternating

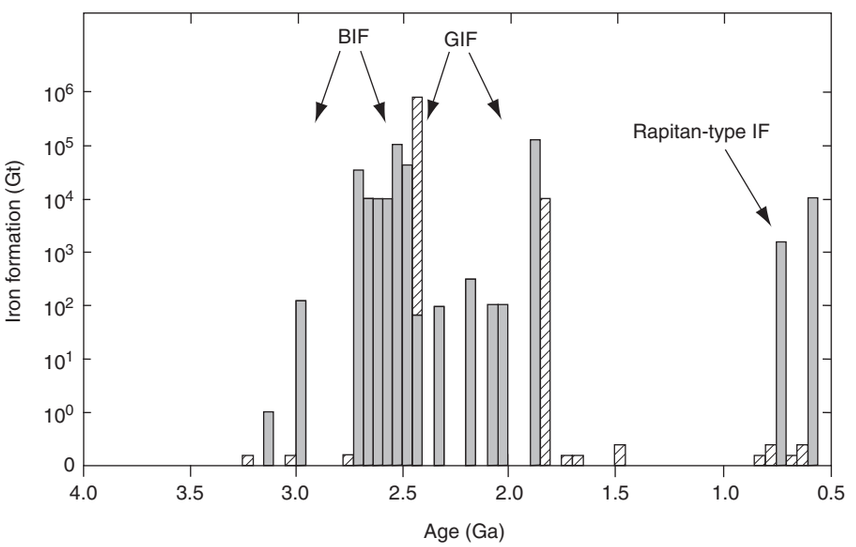

Figure 6.7 Distribution of iron formation deposits over geological time (plotted as time bins of 50 Myr). The diagonal bars indicate significant uncertainty in the age of the iron formation. The Archean and earliest Paleoproterozoic are dominated by deeper-water banded iron formation (BIF), whereas the rest of the Paleoproterozoic is commonly characterized by the deposition of shallower-water granular iron formation (GIF). The change in textural style of iron formation deposition may relate to the first major increase of atmospheric O_2, but is still poorly understood. Neoproterozoic iron formations, often referred to as Rapitan-type after the type locality in northwestern Canada, may be a product of ferruginous oceans during widespread, low-latitude glaciations and/or enhanced hydrothermal Fe(II) inputs to rift basins. Modified from Bekker *et al*. (2010).

(metre- to sub-millimetre-thick) layers of iron-rich minerals and silicate/carbonate minerals, with a typical bulk chemical composition of ~20–40 wt% Fe and ~40–60 wt% SiO_2. Known specifically as banded iron formation (or BIF) because of their layering, some of these BIF (such as those of the Hamersley Group of Western Australia and Transvaal Supergroup of South Africa) that were deposited at the Archean–Paleoproterozoic transition are hundreds of meters thick and formed over vast depositional areas of ~10^5 km^2 (Morris, 1993; Trendall, 2002; Klein, 2005).

It is now widely believed that the ultimate source of the iron in iron formation is Fe(II) from hydrothermal systems (Jacobsen and Pimentel-Klose, 1988; Derry and Jacobsen, 1990; Bau and Möller, 1993) that were located either distally (i.e. from mid-ocean ridges) or proximally (i.e. from shallow submarine volcanoes) to the site of iron formation deposition. Given a distal source, it was suggested that upwelling anoxic waters had Fe(II) concentrations of 40–120 μM, assuming equilibrium with siderite and calcite (Holland, 1984; Canfield, 2005). However, the upwelling rate required to account for iron formation sedimentation rates is approximately an order of magnitude higher than maximum sedimentation rates in modern coastal environments (Konhauser *et al*., 2007a). An origin proximal to hydrothermal plumes is suggested by a correlation between mantle plume activity and iron formation deposition between 3.8 and 1.85 Ga (Isley, 1995; Barley *et al*., 1997, 2005; Isley and Abbott, 1999; Bekker *et al*., 2010).

Anoxic deep oceans would have facilitated transport of Fe(II) from deeper to shallower waters (Cloud, 1968; Holland, 1973). However, the next step – oxidation of Fe(II) to Fe(III) and the precipitation of ferric oxyhydroxides – is where the picture becomes blurry (Fig. 6.8). Three main hypotheses have been proposed for the

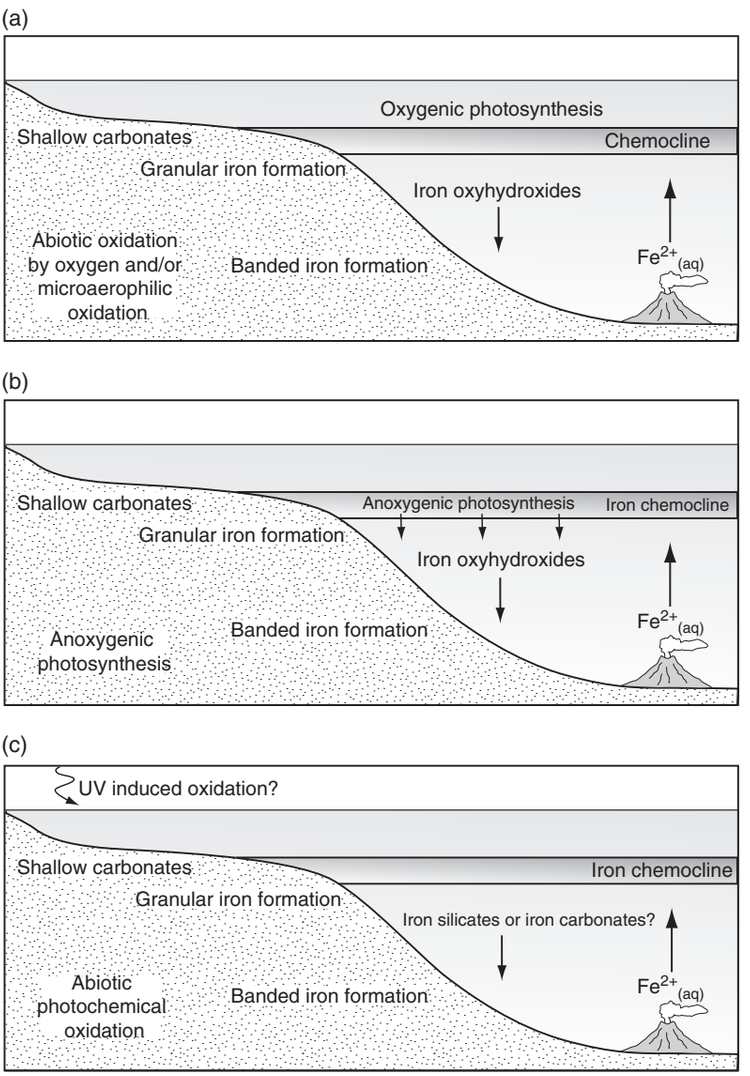

Figure 6.8 Main hypotheses for the mechanism of Fe(II) oxidation necessary for iron formation deposition. (a) Abiotic or microbially catalysed reaction of Fe(II) with dissolved O_2 released during cyanobacterial oxygenic photosynthesis. (b) Direct microbial oxidation during anoxygenic photosynthesis (photoferrotrophy). (c) Abiotic photo-oxidation of dissolved Fe(II) by ultraviolet light. In the vicinity of hydrothermal plumes from shallow submarine volcanoes, photo-oxidation of Fe(II) would likely have been insignificant relative to the formation of ferrous silicate and/or ferrous carbonate minerals. Anoxygenic photosynthesis is suggested to be the dominant oxidation mechanism in the Archean oceans, but the abiotic and/or microbially catalysed oxidation of Fe(II) by O_2 ultimately took on a major role following the evolution of oxygenic photosynthesis. Modified from Bekker *et al*. (2010).

mechanism of Fe(II) oxidation: (1) abiotic or microbially catalysed reaction of Fe(II) with dissolved O_2 released during cyanobacterial oxygenic photosynthesis (Cloud, 1968, 1973); (2) direct microbial oxidation during anoxygenic photosynthesis (photoferrotrophy; Garrels *et al*., 1973; Hartman, 1984; Widdel *et al*., 1993; Konhauser *et al*., 2002; Kappler *et al*., 2005b; Crowe *et al*., 2008), and (3) abiotic photo-oxidation of dissolved Fe(II) by ultraviolet light (Cairns-Smith, 1978; Braterman *et al*., 1983, 1984; François, 1986). Early laboratory experiments demonstrated the plausibility of photochemical Fe(II) oxidation (Anbar and Holland, 1992). Subsequently, experiments by Konhauser *et al*. (2007a) showed that photo-oxidation of Fe(II) in an anoxic Precambrian surface ocean was likely negligible in close proximity to hydrothermal plumes from shallow submarine volcanoes. In these environments, photosynthesis is the leading candidate for providing the oxidant. It is possible that prior to ocean oxygenation, photoferrotrophy was generally the mechanism of choice for producing ferric oxyhydroxides, but at some stage, oxygen played a greater role. The timing of this transition is unresolved.

It has long been postulated that oxygen oases – local regions in the surface ocean where rates of cyanobacterial oxygenic photosynthesis were high enough to permit O_2 accumulation – might have existed before the first major increase in atmospheric O_2 (Kasting, 1993). Hydrocarbon biomarker evidence (2-methylhopanes) from 2.7–2.5 Ga black shales may suggest cyanobacteria had evolved by the Late Archean (Brocks *et al*., 1999, 2003; Summons *et al*., 1999; Eigenbrode *et al*., 2008; Waldbauer *et al*., 2009). However, an indigenous origin for these molecules has been challenged (Brocks *et al*., 2008; Rasmussen *et al*., 2008; Brocks, 2011) and the same biomarkers can be synthesized by anoxygenic photoautotrophs (Rashby *et al*., 2007; Welander *et al*., 2010). Morphological characteristics of some Late Archean stromatolites may suggest that cyanobacteria evolved by 2.7 Ga (Buick, 1992, 2008; Bosak *et al*., 2009). Sterane biomarkers, considered a diagnostic hallmark of O_2-dependent eukaryotes (Summons *et al*., 2006), are also known from Late Archean black shales (Brocks *et al*., 1999, 2003; Waldbauer *et al*., 2009) but the concerns about younger geological and anthropogenic contaminants (Brocks *et al*., 2008; Rasmussen *et al*., 2008; Brocks, 2011) have yet to be fully resolved.

Geochemical signatures in black shales appear to provide a clearer picture of environmental O_2 levels near the end of the Archean Eon. In the Late Archean Mt. McRae Shale (Hamersley Basin, Western Australia) and Ghaap Group (Griqualand West Basin, South Africa), molybdenum and rhenium enrichments together with sulfur, nitrogen, and molybdenum isotope signatures point to the presence of surface ocean O_2 beneath a low-O_2 atmosphere (<0.001% PAL based on MIF of sulfur isotopes; Anbar *et al*., 2007; Kaufman *et al*., 2007; Wille *et al*., 2007; Garvin *et al*., 2009; Godfrey and Falkowski, 2009; Reinhard *et al*., 2009; Duan *et al*., 2010a; Kendall *et al*., 2010). Black shales deposited on the slope of the Campbellrand–Malmani carbonate platform in the Griqualand West Basin contain high rhenium and low molybdenum enrichments which, along with iron speciation data, indicate the presence of dissolved O_2 in bottom waters beneath the photic zone. These same redox proxies show that the mildly oxygenated surface waters gave way to an anoxic deeper ocean (Kendall *et al*., 2010). Collectively, these observations imply that nutrient-rich regions along Late Archean ocean margins were sites of significant O_2 accumulation more than 100 million years before O_2 began to appreciably accumulate in the atmosphere.

Hence, photosynthetic O_2 could have contributed to the precipitation of ferric oxyhydroxides as early as 2.7 Ga (other controversial geological and geochemical evidence may suggest an even earlier origin for oxygenic photosynthesis; e.g. Rosing and Frei, 2004; Hoashi *et al*., 2009; Kato *et al*., 2009; Kerrich and Said, 2011). Arguably, the strongest peak in iron formation deposition occurred at 2.7–2.45 Ga. Although these iron formations have been interpreted as the products of elevated mantle plume activity and hence an increased Fe(II) supply to seawater (e.g. Barley *et al*., 2005; Bekker *et al*., 2010), it is also possible there is a link between iron formation deposition and oxygenic photosynthesis. Such a link would be implausible if during periods of iron formation deposition, photosynthetic O_2 production was retarded by the widespread adsorption of the nutrient phosphorus onto sedimenting ferric oxyhydroxides (Bjerrum and Canfield, 2002). However, Konhauser *et al*. (2007b) subsequently showed that such particles would not constitute a significant phosphorus sink in the silica-rich Archean oceans. Photosynthetic O_2 merits consideration as an oxidant for the precipitation of ferric oxyhydroxides in Late Archean and earliest Paleoproterozoic oceans, though further research, particularly on the spatiotemporal distribution of O_2, is required to elucidate its significance relative to anoxygenic photosynthesis. Rare earth element (REE) data from Archean iron formations suggest that abiotic oxidation of Fe(II) by free oxygen was limited, but permits the possibility that microaerophilic Fe(II) oxidation was an important oxidation mechanism (along with anoxygenic photosynthesis) in the Late Archean oceans (Planavsky *et al*., 2010b).

6.4.4.3 The Paleoproterozoic Great Oxidation Event and its impact on the iron cycle

The Paleoproterozoic Earth witnessed the first major increase in atmospheric O_2 (the Great Oxidation Event),

as marked by several lines of evidence, including the disappearance of MIF of S isotopes between 2.45 and 2.32 Ga (Farquhar *et al*., 2000, 2011; Bekker *et al*., 2004; Guo *et al*., 2009; Johnston, 2011), a significant increase in Cr abundances in iron formations after 2.48 Ga (Konhauser *et al*., 2011b), the appearance of red beds, sediment-hosted stratiform copper deposits, phosphorites, manganese deposits and increasingly abundant oxidized Fe(III) in paleosols between 2.5 and 2.0 Ga (Cloud, 1968; Chandler, 1980; Eriksson and Cheney, 1992; Rye and Holland, 1998; Bekker *et al*., 2004; Canfield, 2005; Holland, 2006; Farquhar *et al*., 2011; Murakami *et al*., 2011; Sekine *et al*., 2011), and a contemporaneous growth in the diversity of minerals driven by the availability of elements in their oxidized forms (Hazen *et al*., 2009; Sverjensky and Lee, 2010). In addition, the appearance of $CaSO_4$-rich evaporites (Chandler, 1988; El Tabakh *et al*., 1999; Melezhik *et al*., 2005; Schröder *et al*., 2008), enhanced expressions of mass-dependent fractionation of sulfur isotopes (e.g. Cameron, 1982; Canfield and Raiswell, 1999; Canfield *et al*., 2000; Bekker *et al*., 2004; Guo *et al*., 2009), and increased molybdenum abundances in euxinic black shales (Scott *et al*., 2008) point to a rise in seawater sulfate and molybdenum concentrations. The most likely explanation is an increase in the oxidative weathering of crustal sulfide minerals and hence the riverine transport of SO_4^{2-} and MoO_4^{2-} to the oceans. Atmospheric O_2 levels rose above 0.001% PAL (required to eliminate the MIF of sulfur isotopes; Pavlov and Kasting, 2002; Farquhar and Wing, 2003) but likely remained at least an order of magnitude below the present level (Canfield, 2005; Holland, 2006).

What was the impact of the Great Oxidation Event on the iron biogeochemical cycle? From the rock record, it appears that deposition of iron formation was limited between ~ 2.4 and 1.9 Ga and large deposits (≥10 000 Gt) are not known from the rock record (Isley and Abbott, 1999; Bekker *et al*., 2010). The connection between the end of large iron formation deposition and the Great Oxidation Event raises an obvious possibility – the rising atmospheric O_2 levels ventilated the deep oceans, leading to a major reduction in the oceanic iron reservoir via the formation of poorly soluble ferric oxyhydroxides (Holland, 2006). However, other explanations can be envisioned that involve the continuation of deep ocean anoxia. The distribution of U–Pb ages from detrital zircons and subduction-related granitoids, together with a paucity of greenstones, tonalite–trondhjemite–granodiorite (TTG) suites, and large igneous provinces (LIPs), points to a widespread slowdown of magmatic activity between 2.45 and 2.20 Ga (Condie *et al*., 2009). Hence, the general absence of iron formation deposition at this time could reflect low hydrothermal Fe(II) inputs to an otherwise anoxic deep ocean. Another possibility is that increased sulfate fluxes to the oceans stimulated larger rates of microbial sulfide production, leading to an expansion of euxinic waters along productive ocean margins (regions with high organic carbon fluxes) and the removal of Fe(II) into insoluble iron sulfide minerals (Canfield, 2005). The global 2.2–2.1 Ga Lomagundi positive carbon isotope excursion is thought to reflect extensive burial of organic carbon and the release of oxidizing power to the environment (Karhu and Holland, 1996). A more oxic surface environment may have substantially increased seawater sulfate concentrations, and hence the rate of microbial hydrogen sulfide production, although pyrite burial and a return to lower oceanic redox conditions could have resulted in a lower seawater sulfate concentration after the Lomagundi event (Schröder *et al*., 2008). Carbon isotope compositions and iron speciation data from Lomagundi-age sedimentary rocks are consistent with ocean stratification, including water column euxinia (Bekker *et al*., 2008; Scott *et al*., 2008).

A final widespread episode of large iron formation deposition at 1.88–1.85 Ga (predominantly as shallow-water granular iron formation, also known as GIF; Bekker *et al*., 2010) indicates a return to Fe(II)-rich deep oceans. This change may be associated with an increase in mantle plume activity (Bekker *et al*., 2010). An alternative (though not mutually exclusive) hypothesis is a decline in atmospheric and hence oceanic O_2 levels. Support for this comes from the occurrences of ferric oxyhydroxide precipitation in high-energy, shallow-water environments, which requires Fe(II) transport from anoxic deeper waters into shallow continental shelves where reaction with photosynthetic O_2 can occur (Canfield, 2005 and references therein). Furthermore, chromium isotope compositions in the 1.9 Gyr-old Gunflint Formation (Ontario, Canada) are not fractionated relative to igneous rocks, suggesting minimal oxidative mobilization of chromium from the upper crust because of a low-O_2 atmosphere (Frei *et al*., 2009).

6.4.4.4 Iron's fall and redemption: The end of large iron formation deposition and the nature of Middle Proterozoic ocean chemistry

With the exception of occurrences commonly associated with low-latitude Neoproterozoic glacial deposits (Hoffman and Schrag, 2002) and sporadic, generally small Middle Proterozoic deposits (Bekker *et al*., 2010), iron formations disappear from the rock record after ~1.85 Ga. This major change in the iron biogeochemical cycle has attracted substantial interest among biogeochemists for the past dozen years. Originally, the disappearance of the large iron formations was attributed to a major rise in atmospheric O_2 concentrations that led to the development of mildly oxygenated and iron-scarce deep oceans (Holland, 1984,

2006). However, Canfield (1998) suggested instead that a smaller atmospheric O_2 increase would allow the persistence of anoxic deep oceans while simultaneously increasing seawater sulfate concentrations to the point where elevated rates of microbial hydrogen sulfide production led to widespread ocean euxinia and the removal of dissolved Fe(II) into iron sulfide minerals.

Several lines of geochemical evidence, particularly iron speciation data, has since been advanced in support of some variant of the 'Canfield' ocean, the most compelling of which was the apparent capture of the transition from ferruginous to euxinic deep ocean conditions at ~1.84 Ga in the Animikie Basin (Lake Superior region; Poulton *et al*., 2004). At least three episodes of deep ocean euxinia were also documented in the 1.8–1.4 Ga McArthur Basin of northern Australia (Shen *et al*., 2002, 2003), including an example of shallow photic zone euxinia indicated by hydrocarbon biomarkers of green and purple sulfur bacteria in the 1.64 Ga Barney Creek Formation (Brocks *et al*., 2005; Brocks and Schaeffer, 2008). Consistent with an expansion of euxinic environments, the end of large iron formation deposition is approximately contemporaneous with the first appearance of exhalative (SEDEX) lead–zinc–sulfide mineralization in the rock record (Lyons *et al*., 2006). Low seawater sulfate concentrations (perhaps ≤1 mM; Canfield *et al*., 2010), inferred from ^{34}S-rich pyrites and rapid variations in the seawater sulfate isotope composition (Lyons *et al*., 2009a and references therein), may fingerprint widespread pyrite burial and the permanent removal of sulfur from the Earth's surface via subduction of the oceanic crust and its sedimentary cover. The return of ferruginous oceans and the increase in iron formation deposition in the Neoproterozoic (Canfield *et al*., 2008) may then reflect the product of extreme sulfate limitation (and hence low rates of microbial hydrogen sulfide production) in a Canfield Ocean that lasted over 1 Gyr (Canfield, 2004).

Was a global expansion of ocean euxinia truly the end of iron's dominance in the deep oceans? Lyons *et al*. (2009a, b) pointed out several problematic issues with the Canfield ocean hypothesis. For example, it is difficult to sustain global euxinia because such conditions should result in widespread depletion of bioessential, redox-sensitive metals (e.g. molybdenum, copper), thereby eradicating the high rates of primary production (which enables high organic carbon export fluxes) required to sustain euxinia. Further, the idea of global deep ocean euxinia is at odds with the molybdenum abundances and isotope compositions of Proterozoic euxinic shales. Because molybdenum burial rates in euxinic environments are high, the molybdenum seawater concentration is sensitive to the extent of euxinic seafloor. Hence, global deep ocean euxinia should easily strip the ocean of nearly all dissolved Mo. However, Proterozoic euxinic shales contain molybdenum enrichments intermediate between that of Archean and Phanerozoic shales, indicating that wholesale drawdown of the Proterozoic oceanic Mo inventory did not occur (Scott *et al*., 2008). Molybdenum isotope data from euxinic shales further supports this contention (Arnold *et al*., 2004; Kendall *et al*., 2009, 2011). The existence of large expanses of oxic or ferruginous seafloor is implied.

If the Middle Proterozoic deep ocean was not globally euxinic, then it must have either contained dissolved O_2 or was still ferruginous. Slack and Cannon (2009) advanced the possibility that a large bolide impact at 1.85 Ga mixed oxic surface waters with anoxic deep waters on a global scale, leading to a new low-O_2 state (~1 μM O_2) for the deep ocean. However, this is a geologically instantaneous event and is unlikely to explain a permanent change in ocean redox chemistry. Independent of the bolide hypothesis, the existence of some low-O_2 regions (<5 μM O_2) in the deep oceans after 1.85 Ga is supported by mineralogical and geochemical data (cerium anomalies) from 1.74–1.71 Ga seafloor-hydrothermal Si–Fe–Mn sedimentary rocks deposited in association with volcanogenic massive sulfides (VMS) (Slack *et al*., 2007, 2009). Sporadic occurrences of oxide-facies, VMS-related exhalites (Slack *et al*., 2007, 2009; Bekker *et al*., 2010) and the absence of Middle Proterozoic marine manganese deposits (anoxic deep-sea conditions are required to permit accumulation of soluble Mn(II); Holland, 2006) are also consistent with a weakly oxygenated deep ocean. Such conditions, if widespread, would have effectively terminated the deposition of large iron formations.

However, recent studies have the potential to bring about a major paradigm shift in our thinking of Middle Proterozoic deep ocean chemistry. By expanding their 2004 study of the 1.9–1.8 Ga Animikie Basin from a single drill core to multiple localities, Poulton *et al*. (2010) sought to elucidate for the first time the paleobathymetric variations in Late Paleoproterozoic ocean chemistry from shallow to deeper waters along a continental margin. Their target: the <1.84 Ga Rove and Virginia Formations which are thought to be deposited after the global cessation of large iron formation deposition (represented in part by the underlying Gunflint Formation). Iron speciation analyses revealed a spatial transition from oxic surface to mid-depth euxinic waters, which in turn gave way to ferruginous deeper waters. Poulton *et al*. (2010) argued that although the deep oceans remained ferruginous, the expansion of water column euxinia along continental margins (perhaps further aided by a diminished ratio of iron to hydrogen sulfide in hydrothermal fluids because of a higher oceanic sulfate concentration; Kump and Seyfried, 2005), was sufficiently widespread to end iron formation deposition. Evidence for ferruginous deep

oceans some tens of millions of years after the end of large iron formation deposition comes in the form of small iron formation deposits, carbonate and clay minerals whose compositions are indicative of iron-rich bottom waters, and Gunflint-type microfossils in the Ashburton Basin of Western Australia (Wilson *et al*., 2010). The lone example of a large deposit after 1.85 Ga is represented by the GIF of the ca. 1.8 Ga Frere Formation (Earaheedy Basin, Western Australia; Pirajno *et al*., 2009).

Younger Middle Proterozoic iron speciation evidence for water column euxinia mostly come from the intracratonic McArthur Basin whose connection to the global ocean was probably restricted to some degree and hence the data from this region may not be representative of open ocean conditions (Lyons *et al*., 2009a). To address this major gap in our understanding of Middle Proterozoic ocean chemistry, Planavsky *et al*. (2011) obtained iron speciation data from mudrocks ranging in age between 1.7 and 1.2 Ga. In all cases, they found abundant evidence for ferruginous deep-ocean conditions in a diverse range of paleogeographic settings, including a passive margin (1.7 Ga Chuanlinggou Formation, northern China), a passive margin that evolved into a foredeep setting (1.2 Ga Borden Basin, Arctic Canada), a restricted extensional setting (1.45 Ga Belt Supergroup, north-central USA), and a continental back-arc environment (1.64 Ga Barney Creek and Lady Loretta formations, northern Australia). A prevalence of ferruginous deep oceans is most harmonious with the Middle Proterozoic occurrences of small iron formation deposits (Bekker *et al*., 2010), available geochemical data (including the inferred molybdenum budget; Lyons *et al*., 2010), and the growing evidence for similar conditions in the Neoproterozoic (Planavsky *et al*., 2011), which we discuss next.

6.4.4.5 Iron's persistent march: the ferruginous Neoproterozoic deep oceans

As mentioned previously, the Neoproterozoic Earth witnessed a return to significant iron formation deposition. The close association of iron formations with low-latitude Neoproterozoic glacial deposits is considered a logical consequence of a global, multi-million-year-long 'Snowball Earth' glaciation because ocean stagnation should lead to a build-up of dissolved Fe(II) in the ice-covered oceans. This idea is further supported by REE signatures, cerium anomalies, and enrichments in iron, manganese, and other redox-sensitive trace elements in post-glacial cap carbonates (e.g., Huang *et al*., 2011). At the end of the glaciation when ocean circulation is re-established, the upwelling of dissolved Fe(II) into oxic shallower waters would drive ferric oxyhydroxide precipitation. This could also occur during the glaciation where ice cover was sufficiently thin to allow oxygenic photosynthesis (Hoffman and Schrag, 2002). Widespread glaciation would also facilitate iron formation deposition by cutting off the supply of riverine sulfate to the oceans and by increasing the iron-to-hydrogen sulfide ratio in hydrothermal fluids via the lowered hydrostatic pressure that would accompany a significant drop in global sea level (Kump and Seyfried, 2005). This latter explanation is also consistent with less severe 'Slushball Earth' glaciations (ice-free equatorial oceans; Fairchild and Kennedy, 2007). The mineralogical simplicity of the iron-bearing phases (predominantly hematite) in Neoproterozoic compared to Archean–Paleoproterozoic iron formations may arise from limited organic carbon delivery to the glaciated oceans, which would have retarded the formation of reduced iron phases during diagenesis (Halverson *et al*., 2011). Others advocate that iron formation deposition was partly or primarily related to enhanced hydrothermal fluxes in restricted rift basins during the breakup of the supercontinent Rodinia (Young, 2002; Eyles and Januszczak, 2004; Bekker *et al*., 2010; Basta *et al*., 2011).

Recently, Canfield *et al*. (2008) presented an impressive compilation of more than 700 iron speciation analyses from 34 different formations and concluded that the Neoproterozoic deep oceans were predominantly ferruginous between ca. 750 and 530 Ma. A similar conclusion was reached for the ca. 800–742 Ma Chuar Group (Johnston *et al*., 2010). Li *et al*. (2010) then provided a detailed picture of Ediacaran ocean chemistry through iron speciation analyses on the 635–551 Ma Doushantuo Formation. They showed that mid-depth euxinic waters were sandwiched within ferruginous deep waters in the Nanhua Basin, South China. Other examples of water column euxinia from the Neoproterozoic were previously noted (Canfield *et al*., 2008; Scott *et al*., 2008; Johnston *et al*., 2010), but Li *et al*. (2010) were the first to clearly delineate the paleobathymetric distribution of euxinic and ferruginous conditions beneath oxic surface waters for a Neoproterozoic continental margin.

Most delightfully, the proposed redox structure for the Middle Proterozoic and Neoproterozoic oceans – oxic surface waters, mid-depth euxinic waters in regions of elevated organic carbon export along productive ocean margins, and ferruginous deeper waters – is very similar (Fig. 6.9; Li *et al*., 2010; Poulton *et al*., 2010; Planavsky *et al*., 2011). Furthermore, this redox structure probably had its roots along Late Archean ocean margins prior to the first major rise in atmospheric O_2 (Reinhard *et al*., 2009; Kendall *et al*., 2010; Scott *et al*., 2011). These recent observations raise the tantalizing possibility that the same basic ocean redox structure has held sway for ~2 Gyr of Earth's middle age (Planavsky *et al*., 2011; Poulton and Canfield, 2011).

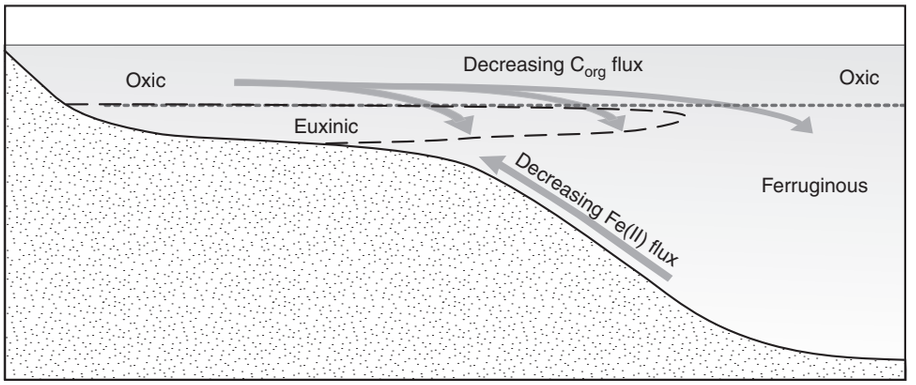

Figure 6.9 Redox conditions in the Proterozoic oceans based on Poulton *et al*. (2010), Li *et al*. (2010) and Planavsky *et al*. (2011). The surface oceans were mildly oxygenated after the initial rise of atmospheric O_2 but the deep oceans were anoxic. At mid-water depths, locally high organic carbon (C_{org}) and sulfate fluxes stimulated extensive microbial hydrogen sulfide production. Anoxic and sulfidic (euxinic) conditions developed when sulfide became sufficiently abundant to quantitatively titrate Fe(II) from the water column through sedimentary pyrite formation. These euxinic waters gave way at depth to anoxic and iron-rich (ferruginous) conditions where Fe(II) still remained in solution after the removal of all sulfide as pyrite. A similar redox structure has been proposed for the Late Archean ocean, with the exception that oxygenated surface waters were confined to the ocean margins. Modified from Poulton *et al*. (2010).

6.4.4.6 Iron dethroned: the transition to fully oxygenated Phanerozoic oceans

Abundant geochemical data point to a second major increase in atmospheric O_2 levels during the late Neoproterozoic (e.g. Des Marais *et al*., 1992; Canfield and Teske, 1996; Hurtgen *et al*., 2005; Fike *et al*., 2006; McFadden *et al*., 2008; Scott *et al*., 2008; Knauth and Kennedy, 2009), but this O_2 rise did not immediately spell the end of iron's reign in the deep oceans. Indeed, it was not until approximately 580 Ma that the first glimmerings of substantial, regionally stable deep-ocean oxygenation appear in the geochemical record. In the Avalon Peninsula of Newfoundland (Canada), iron speciation data appear to capture a transition from ferruginous deep waters before and during the ca. 580 Ma Gaskiers glaciation to oxygenated deep waters that persisted for at least 15 Myr afterwards. The minimum atmospheric O_2 level required to enable this expansion of deep ocean O_2 was calculated to be 15% PAL assuming waters supplying the deep ocean had an oxygen content of at least 50 μM (to account for deep-sea oxygen deficits and aerobic respiration by Ediacaran metazoans; Canfield *et al*., 2007). Similar iron speciation evidence of deep ocean oxygenation was found in late Ediacaran sedimentary rocks of the Windermere Supergroup, Western Canada (Canfield *et al*., 2008; Shen *et al*., 2008). Molybdenum abundances in euxinic black shales increase to Phanerozoic-like levels between 663 and 551 Ma, pointing to a larger dissolved Mo inventory in more extensively oxygenated oceans (Scott *et al*., 2008).

However, the iron speciation evidence for ferruginous deep oceans from other late Ediacaran sections indicates that ocean oxygenation was not global at this time (Canfield *et al*., 2008; Li *et al*., 2010). In fact, geochemical evidence indicates that non-trivial expanses of seafloor remained anoxic to the Precambrian–Cambrian boundary (Canfield *et al*., 2008; Wille *et al*., 2008; Ries *et al*., 2009) and perhaps well into the early Phanerozoic (Goldberg *et al*., 2007; Dahl *et al*., 2010; Gill *et al*., 2011). Elucidating the nature and timing of the transition to predominantly oxygenated and iron-scarce oceans and its significance for metazoan evolution remains a high priority for the biogeochemistry community. Other than enhanced iron transport and scavenging during oceanic anoxic events (Meyer and Kump, 2008) and in restricted anoxic basins (like the modern Black Sea; Lyons and Severmann, 2006; Severmann *et al*., 2008), iron biogeochemical cycling in the near-pervasively oxygenated Phanerozoic oceans was limited primarily to anoxic sediments, particularly the benthic iron flux on continental margins (e.g. Homoky *et al*., 2009; Severmann *et al*., 2010).

6.4.2 Consequences for biology

Iron has likely played a significant role in cellular metabolism since the very first microorganisms appeared on Earth. It has been argued that the very first prebiotic metabolisms occurred in the vicinity of deep-sea hydrothermal vents and coupled the reduction of CO_2 into an anionic carboxylate group using energy from the reaction between FeS (mackinawite) with dissolved H_2S at temperatures of 100°C to form pyrite:

$$FeS + H_2S \rightarrow FeS_2 + H_2 \quad \Delta G^{0'} = -38.4\ \text{kJ mol}^{-1}$$

Importantly, the reaction is exergonic, yielding sufficient free energy for the formation of adenosine triphosphate (ATP) from adenosine diphosphate (ADP), which requires 31.8 kJ mol^{-1} (Drobner *et al*., 1990). Under slightly acidic conditions, and in the presence of dissolved Fe^{2+}, pyrite has a positively-charged surface that would adsorb inorganic anions (i.e. carbonate, sulfide, phosphate) and negatively-charged organic molecules (e.g. Russell and Hall, 1997; Bebié and Schoonen, 1999). These products could then accumulate and polymerize to more complex compounds directly on the pyrite. The central role of iron in those early biochemical reactions may also explain their later incorporation into a number of enzymes, such as Fe–S proteins and cytochromes (Wächtershäuser, 1988).

The generation of H_2 as a by-product from the above reaction would have proven fortuitous because it could eventually have been used as an electron donor in subsequent metabolic reactions, gradually supplementing and then replacing the original energy source when the first primitive hydrogenase activity had evolved (Kandler, 1994). Simultaneously, the electrons would have needed disposing of, and the possible presence of ferric iron on the seafloor due to surface photochemical reactions in the absence of an effective UV screen would have served this purpose nicely:

$$0.5H_2 + Fe(OH)_3 \rightarrow Fe^{2+} + 2OH^- + H_2O$$

There is certainly evidence to suggest that ferric iron was available in the early Archean – the presence of iron formations in the 3.8–3.7 Ga Isua Greenstone Belt in Greenland (Dauphas *et al*. 2004) and the Nuvvuagittuq Supracrustal Belt in northern Québec (Dauphas *et al*., 2007). What is less clear is when Fe(III)-reducing bacteria evolved and took advantage of the ferric iron as an electron donor. Based on the hyperthermophilic lifestyle of some bacteria that are deeply rooted in the phylogenetic tree, it has been suggested that Fe(III) reducers are very old indeed (Vargas *et al*., 1998; Kashefi and Lovley, 2000). Some supporting evidence for an ancient Fe(III) reduction pathway comes from highly negative δ^{56}Fe values in 2.9 Gyr old organic carbon- and magnetite-rich shales (Rietkuil Formation, South Africa; Yamaguchi *et al*., 2005) and 2.7 Gyr old pyrites (Manjeri Formation, Zimbabwe; Archer and Vance, 2006). These δ^{56}Fe values are comparable with the negative fractionations observed from cultures of dissimilatory Fe(III)-reducing (DIR) bacteria (Johnson *et al*., 2005) and in modern ferric oxyhydroxide-rich chemical sediments (Tangalos *et al*., 2010) and the oxic–anoxic boundary of modern ferruginous lakes (Teutsch *et al*., 2009) where DIR is taking place. Recent iron, carbon, and oxygen isotope studies of Late Archean to earliest Paleoproterozoic (2.7–2.45 Ga) sedimentary rocks from South Africa and Western Australia also support a prominent role for DIR (Czaja *et al*., 2010; Heimann *et al*., 2010). Iron and carbon isotope signatures in metacarbonates from iron formation of the Isua Greenstone Belt are similar to those of the Late Archean iron formations, suggesting that DIR is as ancient as the oldest known sedimentary rocks on Earth (Craddock and Dauphas, 2011). Coupling the reduction of Fe(III) minerals to the oxidation of organic matter also explains the low content of organic carbon in iron formations (<0.5%; Gole and Klein, 1981), as well as the abundance of light carbon isotope signatures associated with the interlayered carbonate minerals (Perry *et al*., 1973; Walker, 1984; Baur *et al*., 1985).

The lightest δ^{56}Fe values are observed in sedimentary pyrites and black shales between ~2.7 and 2.5 Ga (Johnson *et al*., 2008). This distinctive isotopic transition may reflect a radiation of DIR (Fig. 6.10). It has been hypothesized that the increased expression of DIR may be coupled to the evolution of oxygenic photosynthesis, which would provide an abundant supply of organic carbon and Fe(III). After the Great Oxidation Event, δ^{56}Fe variability is attenuated, consistent with a decline in open-ocean DIR arising from lower reactive Fe(III) availability in response to the expansion of oxygenated and sulfidic (from increased sulfate availability) waters that remove Fe from solution (Johnson *et al*., 2008).

Alternatively, the light δ^{56}Fe values could reflect the preferential sequestration of heavy iron isotopes onto iron oxyhydroxides during episodes of large iron formation deposition. This would leave seawater with a pool of isotopically light iron, which could subsequently be incorporated into pyrite (Rouxel *et al*., 2005; Anbar and Rouxel, 2007). However, for this process to explain the lightest δ^{56}Fe signatures (–3.5‰) alone, it would require ~90% of the dissolved iron pool to be removed as iron oxyhydroxides, at least episodically. It is likely that both abiotic and DIR-driven iron isotope fractionation played an important role in the Late Archean oceans.

Severmann *et al*. (2008) proposed that a benthic iron flux from continental shelves, made isotopically light by the combined effects of Fe(II) oxidation and DIR, supplied isotopically light iron to seawater. Additional iron isotope fractionation, favouring the uptake of lighter isotopes, could have occurred during pyrite formation in deeper euxinic waters if iron was not quantitatively removed from solution (likely the case because Late Archean oceans were Fe(II)-rich and sulfate-poor). Hence, the light δ^{56}Fe from 2.7–2.5-Gyr-old black shales and pyrites may reflect an increase in the extent of iron redox cycling in response to O_2 accumulation along ocean margins. A fingerprint of DIR's influence on this shelf-to-basin iron 'shuttling' is seen in the distinctive pattern of δ^{56}Fe vs. Fe/Al in recent Black Sea sediments (Severmann *et al*., 2008) and in some Devonian black

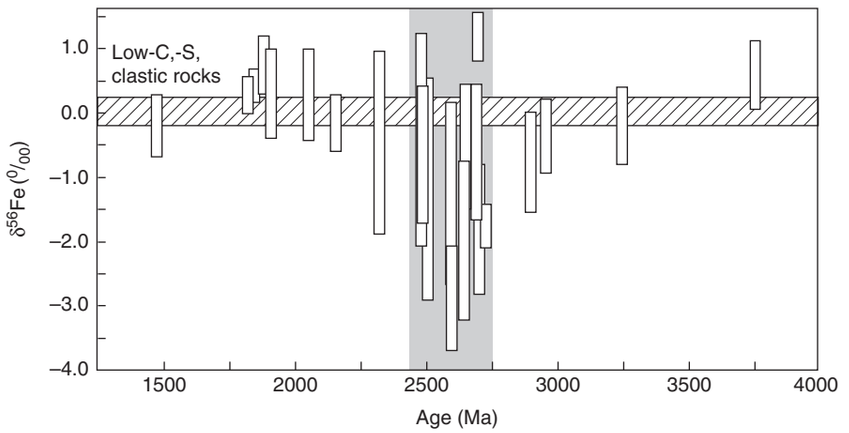

Figure 6.10 Iron isotope compositions of Archean to Middle Proterozoic sedimentary rocks (iron formations and carbon-, sulfur-, and/or iron-rich shales) and sedimentary sulfide minerals. The horizontal bar reflects the typical range in iron isotope composition for organic carbon- and sulfur-poor sedimentary rocks of Archean to Phanerozoic age. Light iron isotope compositions of less than −2‰ are exclusive to the Late Archean (shaded region). Iron isotope compositions are reported as per mil deviations from the average of igneous rocks: $\delta^{56}Fe\ (‰) = [(^{56}Fe/^{54}Fe)_{sample}/(^{56}Fe/^{54}Fe)_{Igneous\ Rocks} - 1] \times 1000$. Modified from Johnson *et al*. (2008).

shales (Duan *et al*., 2010b). A similar pattern is observed in black shales of the 2.5 Ga Mt. McRae Shale (Duan *et al*., 2007). Czaja *et al*. (2010) suggested that in the Late Archean Hamersley Basin, DIR played an important role in providing isotopically light iron to deeper water environments (Jeerinah Formation euxinic shales and Carawine Dolomite carbonates/shales). In contrast, they show that light $\delta^{56}Fe$ signatures of shallow-water carbonates (Wittenoom Formation) were likely a result of Fe(II) oxidation in the photic zone (cf. Rouxel *et al*., 2005; Anbar and Rouxel, 2007). Hence, iron oxyhydroxides fueling DIR could have been isotopically light and together with DIR-related isotope fractionation would have resulted in an amplified light $\delta^{56}Fe$ signature relative to that achieved by either process alone (Severmann *et al*., 2008).

One problem is that a complementary marine sink with heavy $\delta^{56}Fe$ to balance the predominantly light $\delta^{56}Fe$ signatures in Late Archaean sedimentary materials has not been identified. Such a sink could be represented by pelagic sediments, which are not preserved in the geological record (Steinhoefel et al., 2010). However, Guilbaud *et al*. (2011) argued that the need for a heavy $\delta^{56}Fe$ marine sink and a large oceanic pool with light $\delta^{56}Fe$ could be eliminated if the light pyrite $\delta^{56}Fe$ arises from isotope fractionation during abiotic pyrite formation rather than DIR. This hypothesis proposes that a small degree of Fe(II) utilization in iron-rich oceans enabled the full expression of iron isotope fractionation between Fe^{2+}, mackinawite, and pyrite, with minimal impact on the isotopic composition of the remaining oceanic Fe(II) pool. When a substantial proportion of dissolved Fe(II) was depleted via pyrite or oxide mineral formation, as in the Proterozoic and Phanerozoic oceans, then the expression of isotope fractionation became muted, leading to a narrow range of heavier pyrite $\delta^{56}Fe$ (Guilbaud *et al*., 2011).

Nevertheless, microbial processes likely played an important role in the formation of the iron- and silica-rich layers in BIFs. Anoxygenic phototrophic Fe(II) oxidation and microaerophilic Fe(II) oxidation are temperature-dependent microbial processes. Seawater temperature fluctuations in the photic zone may have resulted in repeated cycles of microbially catalysed iron oxyhydroxide deposition and abiotic silica precipitation (Posth *et al*., 2008). Others argue instead for a prominent role of DIR in generating the alkalinity necessary for the precipitation of siderite and for concentrating silica, which was then precipitated as diagenetic minerals (e.g. Fischer and Knoll, 2009; Heimann *et al*., 2010).

With the evolution of photoferrotrophy, biological Fe(II) oxidation would have superseded photochemical oxidation because the bacteria could grow deeper in the water column where UV radiation would be effectively absorbed (Kappler *et al*., 2005b). As long as a source of ferrous iron and nutrients were available, photoferrotrophy could have contributed to ferric iron deposition onto vast areas of seafloor, some of which became manifest as iron formation. What is poorly constrained, however, is when did Fe(II)-based anoxygenic photosynthesis first take place, and how did the photoferrotrophs respond to the evolution and diversification of cyanobacteria in the water column? At present, there is no actual physical or chemical evidence for

photoferrotrophs in the rock record, but a number of independent lines of evidence do suggest their presence on the early Earth. First and foremost, molecular phylogenetic analysis of a number of enzymes involved in (bacterio-)chlorophyll biosynthesis suggests that anoxygenic photosynthetic lineages are almost certain to be more deeply rooted than the oxygenic cyanobacterial lineages (Xiong, 2006). Second, modern anoxygenic phototrophs, including photoferrotrophs, display the ability to utilize multiple substrates such as H_2S, H_2 and Fe(II) (Croal *et al*., 2009). Yet, in the Archean oceans, dissolved sulfide would have been removed from seawater by reacting with the abundant Fe(II) in the deep sea, while available H_2 would have been consumed at depth by methanogenic bacteria (Konhauser *et al*., 2005). By contrast, the input of dissolved Fe(II) from mid-ocean ridges was almost certainly greater during the Archean. Third, the recovery of 2α-methylhopanes from bitumens in the 2.6 Ga Marra Mamba Iron Formation and the 2.5 Ga Mt. McRae Shale (Hamersley Basin) initially led researchers to conclude that oxygenic photosynthesis was already in existence at that time because those biomarkers were considered unique to cyanobacteria (Brocks *et al*., 1999; Summons *et al*., 1999). However, most recently it has been demonstrated that an anoxygenic Fe(II)-oxidizing phototroph, *Rhodopseudomonas palustris*, generates substantial quantities of 2-methylhopanoids in the absence of oxygen (Rashby *et al*., 2007), making the case for Fe(II)-oxidizing phototrophs at 2.6 Ga just as plausible as that for cyanobacteria.

When cyanobacteria eventually did begin to dominate the ocean's photic zones, the oxygen they produced would have allowed other bacteria to begin elaborating on their electron transport chain to include special terminal reductase enzymes that made it possible to pass electrons directly onto O_2. The benefit for those cells was that they could now harness more energy from the inorganic and organic substrates they oxidized. In the case of Fe(II) oxidation, chemolithoautotrophs, such as *Gallionella*, may even have thrived under early low oxygen conditions as they would have enjoyed a kinetic advantage over inorganic or photosynthetic reactions (Holm, 1989). At 1.9–1.8 Ga, Fe(II)-oxidizing bacteria appear to have colonized large tracts of the shallow marine environment where iron-rich deep waters were brought into contact with fully oxygenated surface waters (Planavsky *et al*., 2009; Wilson *et al*., 2010).

6.5 Summary

The central role of iron in modern biology is probably a legacy of the early Earth, when the Archean atmosphere was essentially devoid of O_2 and the anoxic oceans contained abundant dissolved, and thus, bioavailable Fe(II). Iron was likely to have been involved in the first prebiotic metabolic reactions near deep-sea hydrothermal systems. Dissimilatory Fe(III)-reducing bacteria may have had their origins in the Early Archean. Anoxygenic photosynthesis (photoferrotrophy) would likely have been an important metabolic process in the iron-rich oceans and its origin is thought to predate cyanobacterial oxygenic photosynthesis.

Archean and earliest Paleoproterozoic iron formations were probably the direct and indirect products of microbial processes. When O_2 was scarce, anoxygenic photosynthesis may have driven Fe(II) oxidation. With the advent of cyanobacterial O_2 production and accumulation in surface waters, Fe(II)-oxidizing bacteria is likely to have become an important component of microbial ecosystems at the interface between oxic and ferruginous water masses. Hence, microaerophilic Fe(II) oxidation and the abiotic oxidation of Fe(II) by photosynthetically produced O_2 likely played an increasingly important role in the Late Archean oceans. Ultimately, Fe(II) oxidation by O_2 became the principle metabolic process driving the formation of Paleoproterozoic iron formations after the Great Oxidation Event.

Conventional wisdom held that the ferruginous oceans disappeared along with the large iron formations after 1.85 Ga because of the establishment of oxic or euxinic deep oceans in response to rising atmospheric O_2 levels. Recent geochemical studies, however, point to a complex stratification of the oceans during Earth's middle age, with oxic surface waters underlain by mid-depth euxinic waters along productive ocean margins, which in turn gave way to predominantly ferruginous deep oceans. The end of large iron formation deposition at 1.85 Ga may then reflect an expansion of euxinic water masses along ocean margins, which led to the titration of upwelling, dissolved Fe(II) as insoluble sedimentary sulfides. The development of low-O_2 conditions in some regions may also have removed some Fe(II) from solution as iron oxyhydroxides. Nevertheless, ferruginous deep oceans likely continued throughout the rest of the Proterozoic and perhaps into the early Phanerozoic.

Seawater iron concentrations declined dramatically upon the development of the largely oxygenated Phanerozoic oceans because of the poor solubility of iron in the presence of O_2 at the circumneutral pH of seawater. Consequently, the residence time of iron in the oceans became very low, and the biogeochemical cycling of iron was restricted primarily to anoxic sediments. Exceptions to this rule include oceanic anoxic events and restricted anoxic basins. Despite the fact that iron is the limiting nutrient for biological productivity over large parts of the modern ocean, it continues to play a prominent role as a micronutrient and in microbially mediated redox reactions. This is facilitated by the

development of siderophores, which play an important role as Fe(III) chelators that enable bacteria and fungi to satisfy their metabolic requirements when iron is scarce in the environment.

As is the case for other redox-sensitive elements, the story of iron geobiology is one that reflects the planetary co-evolution of life and its environment. Bioavailable iron was plentiful on the anoxic early Earth and may have played an important role in the first metabolisms. Following the advent of cyanobacterial oxygenic photosynthesis, the biogeochemical cycles of iron and oxygen clashed. For much of Earth's middle age, oxygen dominated the surface environments whereas iron continued to play an important role in the ocean depths. Finally, the expansion of O_2 throughout most of the Phanerozoic oceans limited iron biogeochemical cycling to ocean floor sediments, as is observed today.

Acknowledgements

This work was supported by the National Science Foundation, the German Research Foundation (DFG), the Natural Sciences and Engineering Research Council of Canada, the NASA Astrobiology Institute, and the Agouron Institute. Noah Planavsky is thanked for insightful comments that improved the manuscript. We are grateful to Sue Selkirk for drafting the figures.

References

Archer C, Vance D (2006) Coupled Fe and S isotope evidence for Archean microbial Fe(III) and sulfate reduction. *Geology* **34**, 153–156.

Anbar AD, Holland HD (1992) The photochemistry of manganese and the origin of banded iron formations. *Geochimica et Cosmochimica Acta* **56**, 2595–2603.

Anbar A, Rouxel O (2007) Metal stable isotopes in paleoceanography. *Annual Review of Earth and Planetary Sciences* **35**, 717–746.

Anbar AD, Duan Y, Lyons TW, *et al*. (2007) A whiff of oxygen before the Great Oxidation Event? *Science* **317**, 1903–1906.

Arnold GL, Anbar AD, Barling J, Lyons TW (2004) Molybdenum isotope evidence for widespread anoxia in Mid-Proterozoic oceans. *Science* **304**, 87–90.

Barley ME, Pickard AL, Sylvester PJ (1997) Emplacement of a large igneous province as a possible cause of banded iron formation 2.45 billion years ago. *Nature* **385**, 55–58.

Barley ME, Bekker A, Krapež B (2005) Late Archean to Early Paleoproterozoic global tectonics, environmental change and the rise of atmospheric oxygen. *Earth and Planetary Science Letters* **238**, 156–171.

Basta FF, Maurice AE, Fontboté L, Favarger PY (2011) Petrology and geochemistry of the banded iron formation (BIF) of Wadi Karim and Um Anab, Eastern Desert, Egypt: implications for the origin of Neoproterozoic BIF. *Precambrian Research* **187**, 277–292.

Bau M, Möller P (1993) Rare earth element systematics of the chemically precipitated component in Early Precambrian iron formations and the evolution of the terrestrial atmosphere-hydrosphere-lithosphere system. *Geochimica et Cosmochimica Acta* **57**, 2239–2249.

Bauer I, Kappler A (2009) Rates and extent of reduction of Fe(III) compounds and O_2 by humic substances. *Environmental Science & Technology* **43**, 4902–4908.

Baur ME, Hayes JM, Studley SA, Walter MR (1985) Millimeter-scale variations of stable isotope abundances in carbonates from banded iron-formations in the Hamersley Group of Western Australia. *Economic Geology* **80**, 270–282.

Bebié J, Schoonen MAA (1999) Pyrite and phosphate in anoxia and an origin-of-life hypothesis. *Earth and Planetary Science Letters* **171**, 1–5.

Bebout BM, Fitzpatrick MW, Paerl HW (1993) Identification of the sources of energy for nitrogen fixation and physiological characterization of nitrogen-fixing members of a marine microbial mat community. *Applied and Environmental Microbiology* **59**, 1495–1503.

Bekker A, Holland HD, Wang PL, *et al*. (2004) Dating the rise of atmospheric oxygen. *Nature* **427**, 117–120.

Bekker A, Holmden C, Beukes NJ, Kenig F, Eglinton B, Patterson WP (2008) Fractionation between inorganic and organic carbon during the Lomagundi (2.22–2.1 Ga) carbon isotope excursion. *Earth and Planetary Science Letters* **271**, 278–291.

Bekker A, Slack JF, Planavsky N, *et al*. (2010) Iron formation: the sedimentary product of a complex interplay among mantle, tectonic, oceanic, and biospheric processes. *Economic Geology* **105**, 467–508.

Bennett SA, Achterberg EP, Connelly DP, Statham PJ, Fones GR, German CR (2008) The distribution and stabilisation of dissolved Fe in deep-sea hydrothermal plumes. *Earth and Planetary Science Letters* **270**, 157–167.

Berner RA (1970) Sedimentary pyrite formation. *American Journal of Science* **268**, 1–23.

Berner RA (1984) Sedimentary pyrite formation: an update. *Geochimica et Cosmochimica Acta* **48**, 605–615.

Bjerrum CJ, Canfield DE (2002) Ocean productivity before about 1.9 Gyr ago limited by phosphorus adsorption onto iron oxides. *Nature* **417**, 159–162.

Blake R, Johnson DB (2000) Phylogenetic and biochemical diversity among acidophilic bacteria that respire on iron. In: *Environmental Microbe–Metal Interactions* (ed Lovley D). American Society of Microbiology Press, Washington, DC, pp. 53–78.

Blöthe M, Roden EE (2009) Composition and activity of an autotrophic Fe(II)-oxidizing, nitrate-reducing enrichment culture. *Applied and Environmental Microbiology* **75**, 6937–6940.

Bosak T, Liang B, Sim MS, Petroff AP (2009) Morphological record of oxygenic photosynthesis in conical stromatolites. *Proceedings of the National Academy of Sciences* **106**, 10939–10943.

Boyd PW, Ellwood MJ (2010) The biogeochemical cycle of iron in the ocean. *Nature Geoscience* **3**, 675–682.

Boye M, van den Berg CMG, de Jong JTM, Leach H, Croot P, de Baar HJW (2001) Organic complexation of iron in the Southern Ocean. *Deep-Sea Research I* **48**, 1477–1497.

Braterman PS, Cairns-Smith AG, Sloper RW (1983) Photooxidation of hydrated Fe^{2+}-significance for banded iron formations. *Nature* **303**, 163–164.

Braterman PS, Cairns-Smith AG, Sloper RW (1984) Photo-oxidation of iron(II) in water between pH 7.4 and 4.0. *Journal of the Chemical Society, Dalton Transactions: Inorganic Chemistry*, 1441–1445.

Brocks JJ (2011) Millimeter-scale concentration gradients of hydrocarbons in Archean shales: live-oil escape or fingerprint of contamination? *Geochimica et Cosmochimica Acta* **75**, 3196–3213.

Brocks JJ, Schaeffer P (2008) Okenane, a biomarker for purple sulfur bacteria (Chromatiaceae), and other new carotenoid derivatives from the 1640 Ma Barney Creek Formation. *Geochimica et Cosmochimica Acta* **72**, 1396–1414.

Brocks JJ, Logan GA, Buick R, Summons RE (1999) Archean molecular fossils and the early rise of eukaryotes. *Science* **285**, 1033–1036.

Brocks JJ, Buick R, Summons RE, Logan GA (2003) A reconstruction of Archean biological diversity based on molecular fossils from the 2.78 to 2.45 billion-year old Mount Bruce Supergroup, Hamersley Basin, Western Australia. *Geochimica et Cosmochimica Acta* **67**, 4321–4335.

Brocks JJ, Love GD, Summons RE, Knoll AH, Logan GA, Bowden SA (2005) Biomarker evidence for green and purple sulphur bacteria in a stratified Palaeoproterozoic sea. *Nature* **437**, 866–870.

Brocks JJ, Grosjean E, Logan GA (2008) Assessing biomarker syngeneity using branched alkanes with quaternary carbon (BAQCs) and other plastic contaminants. *Geochimica et Cosmochimica Acta* **72**, 871–888.

Buick R (1992) The antiquity of oxygenic photosynthesis: evidence from stromatolites in sulphate-deficient Archaean lakes. *Nature* **255**, 74–77.

Buick R (2008) When did oxygenic photosynthesis evolve? *Philosophical Transactions of the Royal Society B* **363**, 2731–2743.

Buresh RJ, Moraghan JT (1976) Chemical reduction of nitrate by ferrous iron. *Journal of Environmental Quality* **5**, 320–325.

Caccavo F Jr, Schamberger PC, Keiding K, Nielsen PH (1997) Role of hydrophobicity in adhesion of the dissimilatory Fe(III)-reducing bacterium *Shewanella alga* to amorphous Fe(III) oxide. *Applied and Environmental Microbiology* **63**, 3837–3843.

Cairns-Smith AG (1978) Precambrian solution photochemistry, inverse segregation, and banded iron formations. *Nature* **276**, 807–808.

Cameron EM (1982) Sulphate and sulphate reduction in early Precambrian oceans. *Nature* **296**, 145–148.

Canfield DE (1998) A new model for Proterozoic ocean chemistry. *Nature* **396**, 450–453.

Canfield DE (2004) The evolution of the Earth surface sulfur reservoir. *American Journal of Science* **304**, 839–861.

Canfield DE (2005) The early history of atmospheric oxygen. *Annual Review of Earth and Planetary Sciences* **33**, 1–36.

Canfield DE, Raiswell R (1999) The evolution of the sulfur cycle. *American Journal of Science* **299**, 697–723.

Canfield DE, Teske A (1996) Late Proterozoic rise in atmospheric oxygen concentration inferred from phylogenetic and sulphur-isotope studies. *Nature* **382**, 127–132.

Canfield DE, Habicht KS, Thamdrup B (2000) The Archean sulfur cycle and the early history of atmospheric oxygen. *Science* **288**, 658–661.

Canfield DE, Poulton SW, Narbonne GM (2007) Late-Neoproterozoic deep-ocean oxygenation and the rise of animal life. *Science* **315**, 92–95.

Canfield DE, Poulton SW, Knoll AH, *et al*. (2008) Ferruginous conditions dominated later Neoproterozoic deep-water chemistry. *Science* **321**, 949–952.

Canfield DE, Farquhar J, Zerkle AL (2010) High isotope fractionations during sulfate reduction in a low-sulfate euxinic ocean analog. *Geology* **38**, 415–418.

Chan CS, De Stasio G, Welch SA, *et al*. (2004) Microbial polysaccharides template assembly of nanocrystal fibers. *Science* **303**, 1656–1658.

Chandler FW (1980) Proterozoic red bed sequences of Canada. *Geological Survey of Canada Bulletin* **311**, 1–53.

Chandler FW (1988) Diagenesis of sabkha-related, sulphate nodules in the early Proterozoic Gordon Lake Formation, Ontario, Canada. *Carbonates and Evaporites* **3**, 75–94.

Childers SE, Ciufo S, Lovley DR (2002) *Geobacter metallireducens* accesses insoluble Fe(III) oxide by chemotaxis. *Nature* **416**, 767–769.

Chu NC, Johnson CM, Beard, BL, *et al*. (2006) Evidence for hydrothermal venting in Fe isotope compositions of the deep Pacific Ocean through time. *Earth and Planetary Science Letters* **245**, 202–217.

Cloud PE (1968) Atmospheric and hydrospheric evolution on the primitive Earth. *Science* **160**, 729–736.

Cloud PE (1973) Paleoecological significance of the banded iron-formation. *Economic Geology and the Bulletin of the Society of Economic Geologists* **68**, 1135–1143.

Coleman ML (1985) Geochemistry of diagenetic non-silicate minerals: kinetic considerations. *Philosophical Transactions of the Royal Society of London A* **315**, 39–56.

Condie KC, O'Neill C, Aster RC (2009) Evidence and implications for a widespread magmatic shutdown for 250 Myr on Earth. *Earth and Planetary Science Letters* **282**, 294–298.

Craddock PR, Dauphas N (2011) Iron and carbon isotope evidence for microbial iron respiration throughout the Archean. *Earth and Planetary Science Letters* **303**, 121–132.

Croal LR, Johnson CM, Beard BL, Newman DK (2004) Iron isotope fractionation by Fe(II)-oxidizing photoautotrophic bacteria. *Geochimica et Cosmochimica Acta* **68**, 1227–1242.

Croal LR, Jiao Y, Kappler A, Newman DK (2009) Phototrophic Fe(II) oxidation in the presence of H_2: implications for banded iron formations. *Geobiology* **7**, 21–24.

Crowe SA, Jones C, Katsev S, *et al*. (2008) Photoferrotrophs thrive in an Archean Ocean analogue. *Proceedings of the National Academy of Sciences* **105**, 15938–15943.

Cullen JT, Bergquist BA, Moffett JW (2006) Thermodynamic characterization of the partitioning of iron between soluble and colloidal species in the Atlantic Ocean. *Marine Chemistry* **98**, 295–303.

Czaja AD, Johnson CM, Beard BL, Eigenbrode JL, Freeman KH, Yamaguchi KE (2010) Iron and carbon isotope evidence for ecosystem and environmental diversity in the ~ 2.7 to 2.5 Ga Hamersley Province, Western Australia. *Earth and Planetary Science Letters* **292**, 170–180.

Dahl TW, Hammarlund EU, Anbar AD, Bond DPG, Gill BC, Gordon GW, Knoll AH, Nielsen AT, Schovsbo NH, Canfield DE (2010). Devonian rise in atmospheric oxygen correlated to the radiations of terrestrial plants and large predatory fish. *Proceedings of the National Academy of Sciences* **107**, 17911–17915.

Dai MH, Martin JM (1995) First data on trace metal level and behaviour in two major Arctic river-estuarine systems (Ob

and Yenisey) and in the adjacent Kara Sea, Russia. *Earth and Planetary Science Letters* **131**, 127–141.

Dauphas N, van Zuilen M, Wadhwa M, Davis AM, Marty B, Janney PE (2004) Clues from Fe isotope variations on the origin of Early Archean BIFs from Greenland. *Science* **306**, 2077–2080.

Dauphas N, Cates NL, Mojzsis SJ, Busigny V (2007) Identification of chemical sedimentary protoliths using iron isotopes in the >3750 Ma Nuvvuagittuq supracrustal belt, Canada. *Earth and Planetary Science Letters* **254**, 358–376.

Derry LA, Jacobsen SB (1990) The chemical evolution of Precambrian seawater: evidence from REEs in banded iron formation. *Geochimica et Cosmochimica Acta* **54**, 2965–2977.

Des Marais DJ, Strauss H, Summons RE, Hayes JM (1992) Carbon isotope evidence for the stepwise oxidation of the Proterozoic environment. *Nature* **359**, 605–609.

Drobner E, Huber H, Stetter KO (1990) *Thiobacillus ferrooxidans*, a facultative hydrogen oxidizer. *Applied and Environmental Microbiology* **56**, 2922–2923.

Duan Y, Anbar AD, Arnold GL, Gordon GW, Severmann S, Lyons TW (2007) The iron isotope variations in the ~2.5 Ga Mt. McRae Shale. *Geological Society of America Abstracts with Programs* **39**, 449.

Duan Y, Anbar AD, Arnold GL, Lyons TW, Gordon GW, Kendall B (2010a) Molybdenum isotope evidence for mild environmental oxygenation before the Great Oxidation Event. *Geochimica et Cosmochimica Acta* **74**, 6655–6668.

Duan Y, Severmann S, Anbar AD, Lyons TW, Gordon GW, Sageman BB (2010b) Isotopic evidence for Fe cycling and repartitioning in ancient oxygen-deficient settings: examples from black shales of the mid- to late Devonian Appalachian basin. *Earth and Planetary Science Letters* **290**, 244–253.

Edwards KJ, Rogers DR, Wirsen CO, McCollom TM (2003) Isolation and characterization of novel psychrophilic, neutrophilic, Fe-oxidizing, chemolithoautotrophic alpha- and, gamma-Proteobacteria from the deep sea. *Applied and Environmental Microbiology* **69**, 2906-2913.

Eigenbrode JL, Freeman KH, Summons RE (2008) Methylhopane hydrocarbon biomarkers in Hamersley Province sediments provide evidence for Neoarchean aerobiosis. *Earth and Planetary Science Letters* **273**, 323–331.

El-Nagger MY, Wanger G, Leung KM, *et al*. (2010) Electrical transport along bacterial nanowires from *Shewanella oneidensis* MR-1. *Proceedings of the National Academy of Sciences* **107**, 18127–18131.

El Tabakh M, Grey K, Pirajno F, Schreiber BC (1999) Pseudomorphs after evaporitic minerals interbedded with 2.2 Ga stromatolites of the Yerriba basin, Western Australia: origin and significance. *Geology* **27**, 871–874.

England GL, Rasmussen B, Krapez B, Groves DI (2002) Palaeoenvironmental significance of rounded pyrite in siliciclastic sequences of the Late Archean Witwatersrand Basin: oxygen-deficient atmosphere or hydrothermal alteration? *Sedimentology* **49**, 1133–1156.

Eriksson PG, Cheney ES (1992) Evidence for the transition to an oxygen-rich atmosphere during the evolution of red beds in the Lower Proterozoic sequences of southern Africa. *Precambrian Research* **54**, 257–269.

Eyles N, Januszczak N (2004) 'Zipper-rift': a tectonic model for Neoproterozoic glaciations during the breakup of Rodinia after 750 Ma. *Earth-Science Reviews* **65**, 1–73.

Fairchild IJ, Kennedy MJ (2007) Neoproterozoic glaciation in the Earth system. *Journal of the Geological Society, London* **164**, 895–921.

Farquhar J, Wing BA (2003) Multiple sulfur isotopes and the evolution of the atmosphere. *Earth and Planetary Science Letters* **213**, 1–13.

Farquhar J, Bao H, Thiemens M (2000) Atmospheric influence of Earth's earliest sulfur cycle. *Science* **289**, 756–758.

Farquhar J, Peters M, Johnston DT, *et al*. (2007) Isotopic evidence for Mesoarchean anoxia and changing atmospheric sulphur chemistry. *Nature* **449**, 706–709.

Farquhar J, Zerkle AL, Bekker A (2011) Geological constraints on the origin of oxygenic photosynthesis. *Photosynthesis Research* **107**, 11–36.

Fay P, Stewart WDP, Walsby AE, Fogg GE (1968) Is the heterocyst the site of nitrogen fixation in blue-green algae? *Nature* **220**, 810–812.

Fehr MA, Andersson PS, Hålenius U, Gustafsson Ö, Mörth CM (2010) Iron enrichments and Fe isotope compositions of surface sediments from the Gotland Deep, Baltic Sea. *Chemical Geology* **277**, 310–322.

Fike DA, Grotzinger JP, Pratt LM, Summons RE (2006) Oxidation of the Ediacaran ocean. *Nature* **444**, 744–747.

Fischer WW, Knoll AH (2009) An iron shuttle for deepwater silica in Late Archean and early Paleoproterozoic iron formation. *Geological Society of America Bulletin* **121**, 222–235.

Fleet ME (1998) Detrital pyrite in Witwatersrand gold reefs: x-ray diffraction evidence and implications for atmospheric evolution. *Terra Nova* **10**, 302–306.

François LM (1986) Extensive deposition of banded iron formations was possible without photosynthesis. *Nature* **320**, 352–354.

Frei R, Gaucher C, Poulton SW, Canfield DE (2009) Fluctuations in Precambrian atmospheric oxygenation recorded by chromium isotopes. *Nature* **461**, 250–253.

Froelich PN, Klinkhammer GP, Bender ML, *et al*. (1979) Early oxidation of organic matter in pelagic sediments of the eastern equatorial Atlantic: suboxic diagenesis. *Geochimica et Cosmochimica Acta* **43**, 1075–1090.

Garrels RM, Perry EA Jr, MacKenzie FT (1973) Genesis of Precambrian iron-formations and the development of atmospheric oxygen. *Economic Geology* **68**, 1173–1179.

Garvin J, Buick R, Anbar AD, Arnold GL, Kaufman AJ (2009) Isotopic evidence for an aerobic nitrogen cycle in the latest Archean. *Science* **323**, 1045–1048.

Gill BC, Lyons TW, Young SA, Kump LR, Knoll AH, Saltzman MR (2011) Geochemical evidence for widespread euxinia in the Later Cambrian ocean. *Nature* **469**, 80–83.

Godfrey LV, Falkowski PG (2009) The cycling and redox state of nitrogen in the Archaean ocean. *Nature Geoscience* **2**, 725–729.

Goldberg T, Strauss H, Guo Q, Liu C (2007) Reconstructing marine redox conditions for the early Cambrian Yangtze platform: evidence from biogenic sulphur and organic carbon isotopes. *Palaeogeography, Palaeoclimatology, Palaeoecology* **254**, 175–193.

Gole MJ, Klein C (1981) Banded iron-formations through much of Precambrian time. *Journal of Geology* **89**, 169–183.

Gorby YA, Yanina S, McLean JS, *et al*. (2006) Electrically conductive bacterial nanowires produced by *Shewanella oneiden-*

sis strain MR-1 and other microorganisms. *Proceedings of the National Academy of Sciences* **103**, 11358–11363.

Guilbaud R, Butler IB, Ellam RM (2011) Abiotic pyrite formation produces a large Fe isotope fractionation. *Science* **332**, 1548–1551.

Guo Q, Strauss H, Kaufman AJ, *et al* (2009) Reconstructing Earth's surface oxidation across the Archean-Proterozoic transition. *Geology* **37**, 399–402.

Gustafsson O, Widerlund A, Andersson PS, Ingri J, Roos P, Ledin A (2000) Colloid dynamics transport of major elements through a boreal river-brackish bay mixing zone. *Marine Chemistry* **71**, 1–21.

Hallbeck L, Pedersen K (1990) Culture parameters regulating stalk formation and growth rate of *Gallionella ferruginea*. *Journal of General Microbiology* **136**, 1675–1680.

Hallbeck L, Pedersen K (1991) Autotrophic and mixotrophic growth of *Gallionella ferruginea*. *Journal of General Microbiology* **137**, 2657–2661.

Halverson GP, Poitrasson F, Hoffman PF, *et al*. (2011) Fe isotope and trace element geochemistry of the Neoproterozoic synglacial Rapitan iron formation. *Earth and Planetary Science Letters* **309**, 100–112.

Hanert HH (1992) The genus *Gallionella*. In: *The Prokaryotes* (ed Balows A), 2nd edn. Springer, Berlin, pp. 4082–4088.

Hartman H (1984) The evolution of photosynthesis and microbial mats: a speculation on banded iron formations. In: *Microbial Mats: Stromatolites* (eds Cohen Y, Castenholz RW, Halvorson HO). Alan Liss, New York, pp. 451–453.

Hazen RM, Ewing RC, Sverjensky DA (2009) Evolution of uranium and thorium minerals. *American Mineralogist* **94**, 1293–1311.

Hegler F, Posth NR, Jiang J, Kappler A (2008) Physiology of phototrophic iron(II)-oxidizing bacteria – implications for modern and ancient environments. *FEMS Microbiology Ecology* **66**, 250–260.

Hegler F, Schmidt C, Schwarz H, Kappler A (2010) Does a low pH-microenvironment around phototrophic Fe^{II}-oxidizing bacteria prevent cell encrustation by Fe^{III} minerals? *FEMS Microbiology Ecology* **74**, 592–600.

Heimann A, Johnson CM, Beard BL, *et al*. (2010) Fe, C, and O isotope compositions of banded iron formation carbonates demonstrate a major role for dissimilatory iron reduction in ~2.5 Ga marine environments. *Earth and Planetary Science Letters* **294**, 8–18.

Hersman LE, Huang A, Maurice PA, Forsythe JH (2000) Siderophore production and iron reduction by *Pseudomonas mendocina* in response to iron deprivation. *Geomicrobiology Journal* **17**, 261–273.

Hider RC (1984) Siderophore mediated absorption of iron. *Structure and Bonding* **58**, 25–87.

Hoashi M, Bevacqua DC, Otake T, *et al*. (2009) Primary haematite formation in an oxygenated sea 3.46 billion years ago. *Nature Geoscience* **2**, 301–306.

Hofmann AW (1988) Chemical differentiation of the Earth: the relationship between mantle, continental crust, and oceanic crust. *Earth and Planetary Science Letters* **90**, 297–314.

Hoffman PF, Schrag DP (2002) The snowball Earth hypothesis: testing the limits of global change. *Terra Nova* **14**, 129–155.

Hofmann A, Bekker A, Rouxel O, Rumble D, Master S (2009) Multiple sulphur and iron isotope composition of detrital pyrite in Archaean sedimentary rocks: a new tool for provenance analysis. *Earth and Planetary Science Letters* **286**, 436–445.

Holland HD (1973) The oceans: a possible source of iron in iron formations. *Economic Geology and the Bulletin of the Society of Economic Geologists* **68**, 1169–1172.

Holland HD (1984) *The Chemical Evolution of the Atmosphere and Oceans*. Princeton University Press, Princeton, NJ.

Holland HD (2006) The oxygenation of the atmosphere and oceans. *Philosophical Transactions of the Royal Society B* **361**, 903–915.

Holm NG (1989) The $^{13}C/^{12}C$ ratios of siderite and organic matter of a modern metalliferous hydrothermal sediment and their implications for banded iron formations. *Chemical Geology* **77**, 41–45.

Homoky WB, Severmann S, Mills RA, Statham PJ, Fones GR (2009) Pore-fluid Fe isotopes reflect the extent of benthic Fe redox cycling: evidence from continental shelf and deep-sea sediments. *Geology* **37**, 751–754.

Huang J, Chu X, Jiang G, Feng L, Chang H (2011) Hydrothermal origin of elevated iron, manganese and redox-sensitive trace elements in the *c*. 635 Ma Doushantuo cap carbonate. *Journal of the Geological Society, London* **168**, 805–815.

Hurtgen MT, Arthur MA, Halverson GP (2005) Neoproterozoic sulfur isotopes, the evolution of microbial sulfur species, and the burial efficiency of sulfide as sedimentary pyrite. *Geology* **33**, 41–44.

Hutchins DA, Bruland KW (1998) Iron-limited diatom growth and Si:N uptake ratios in a coastal upwelling regime. *Nature* **393**, 561–564.

Isley AE (1995) Hydrothermal plumes and the delivery of iron to banded iron formation. *Journal of Geology* **103**, 169–185.

Isley AE, Abbott DH (1999) Plume-related mafic volcanism and the deposition of banded iron formation. *Journal of Geophysical Research* **104**, 15461–15477.

Jacobsen SB, Pimentel-Klose MR (1988) A Nd isotopic study of the Hamersley and Michipicoten banded iron formations: the source of REE and Fe in Archean oceans. *Earth and Planetary Science Letters* **87**, 29–44.

Javoy M, Kaminski E, Guyot F, *et al*. (2010) The chemical composition of the Earth: enstatite chondrite models. *Earth and Planetary Science Letters* **293**, 259–268.

Jiang J, Kappler A (2008) Kinetics and thermodynamics of microbial and chemical reduction of humic substances: implications for electron shuttling in natural environments. *Environmental Science & Technology* **42**, 3563–3569.

Jiao Y, Newman, DK (2007) The pio operon is essential for phototrophic Fe(II) oxidation in *Rhodopseudomonas palustris* TIE-1. *Journal of Bacteriology* **189**, 1765–1773.

Jickells TD, An ZS, Andersen KK, *et al*. (2005) Global iron connections between desert dust, ocean biogeochemistry, and climate. *Science* **308**, 67–71.

Johnson KS, Gordon RM, Coale KH (1997) What controls dissolved iron concentrations in the world ocean? *Marine Chemistry* **57**, 137–161.

Johnson CM, Roden EE, Welch SA, Beard BL (2005) Experimental constraints on Fe isotope fractionation during magnetite and Fe carbonate formation coupled to dissimilatory hydrous ferric oxide reduction. *Geochimica et Cosmochimica Acta* **69**, 963–993.

Johnson CM, Beard BL, Roden EE (2008) The iron isotope fingerprints of redox and biogeochemical cycling in modern and ancient Earth. *Annual Review of Earth and Planetary Sciences* **36**, 457–493.

Johnston DT (2011) Multiple sulfur isotopes and the evolution of Earth's surface sulfur cycle. *Earth-Science Reviews* **106**, 161–183.

Johnston DT, Poulton SW, Dehler C, *et al*. (2010) An emerging picture of Neoproterozoic ocean chemistry: insights from the Chuar Group, Grand Canyon, USA. *Earth and Planetary Science Letters* **290**, 64–73.

Kandler O (1994) The early diversification of life. In: *Early Life on Earth* (ed Bengtson S). Nobel Symposium No. 84. Columbia University Press, New York, pp. 152–161.

Kappler A, Newman DK (2004) Formation of Fe(III)-minerals by Fe(II)-oxidizing photoautotrophic bacteria. *Geochimica et Cosmochimica Acta* **68**, 1217–1226.

Kappler A, Schink B, Newman DK (2005a) Fe(III)-mineral formation and cell encrustation by the nitrate-dependent Fe(II)-oxidizer strain BoFeN1. *Geobiology* **3**, 235–245.

Kappler A, Pasquero C, Konhauser KO, Newman DK (2005b) Deposition of banded iron formations by anoxygenic phototrophic Fe(II)-oxidizing bacteria. *Geology* **33**, 865–868.

Kappler A, Johnson CM, Crosby HA, Beard BL, Newman DK (2010) Evidence for equilibrium iron isotope fractionation by nitrate-reducing iron(II)-oxidizing bacteria. *Geochimica et Cosmochimica Acta* **74**, 2826–2842.

Karhu JA, Holland HD (1996) Carbon isotopes and the rise of atmospheric oxygen. *Geology* **24**, 867–870.

Kashefi K, Lovley DR (2000) Reduction of Fe(III), Mn(IV), and toxic metals at 100°C by *Pyrobaculum islandicum*. *Applied and Environmental Microbiology* **66**, 1050–1056.

Kasting JF (1993) Earth's early atmosphere. *Science* **259**, 920–926.

Kato Y, Suzuki K, Nakamura K, *et al*. (2009) Hematite formation by oxygenated groundwater more than 2.76 billion years ago. *Earth and Planetary Science Letters* **278**, 40–49.

Kaufman AJ, Johnston DT, Farquhar J, *et al*. (2007) Late Archean biospheric oxygenation and atmospheric evolution. *Science* **317**, 1900–1903.

Kendall B, Creaser RA, Gordon GW, Anbar AD (2009) Re-Os and Mo isotope systematics of black shales from the Middle Proterozoic Velkerri and Wollogorang Formations, McArthur Basin, northern Australia. *Geochimica et Cosmochimica Acta* **73**, 2534–2558.

Kendall B, Reinhard CT, Lyons TW, Kaufman AJ, Poulton SW, Anbar AD (2010) Pervasive oxygenation along late Archean ocean margins. *Nature Geoscience* **3**, 647–652.

Kendall B, Gordon GW, Poulton SW, Anbar AD (2011) Molybdenum isotope constraints on the extent of late Paleoproterozoic ocean euxinia. *Earth and Planetary Science Letters* **307**, 450–460.

Kerrich R, Said N (2011) Extreme positive Ce-anomalies in a 3.0 Ga submarine volcanic sequence, Murchison Province: oxygenated marine bottom waters. *Chemical Geology* **280**, 232–241.

Khan A, Connolly JAD, Taylor SR (2008) Inversion of seismic and geodetic data for the major element chemistry and temperature of the Earth's mantle. *Journal of Geophysical Research* **113**, B09308.

Klein C (2005) Some Precambrian banded iron formations (BIFs) from around the world: their age, geologic setting, mineralogy, metamorphism, geochemistry, and origin. *American Mineralogist* **90**, 1473–1499.

Knauth LP, Kennedy MJ (2009) The late Precambrian greening of the Earth. *Nature* **460**, 728–732.

Konhauser KO, Hamade T, Raiswell R, *et al*. (2002) Could bacteria have formed the Precambrian banded iron formations? *Geology* **30**, 1079–1082.

Konhauser KO, Newman DK, Kappler A (2005) The potential significance of microbial Fe(III)-reduction during Precambrian banded iron formations. *Geobiology* **3**, 167–177.

Konhauser KO, Amskold L, Lalonde SV, Posth NR, Kappler A, Anbar A (2007a) Decoupling photochemical Fe(II) oxidation from shallow-water BIF deposition. *Earth and Planetary Science Letters* **258**, 87–100.

Konhauser KO, Lalonde SV, Amskold L, Holland HD (2007b). Was there really an Archean phosphate crisis? *Science* **315**, 1234.

Konhauser KO, Pecoits E, Lalonde SV, *et al*. (2009) Oceanic nickel depletion and a methanogen famine before the Great Oxidation Event. *Nature* **458**, 750–753.

Konhauser KO, Kappler A, Roden EE (2011a) Iron in microbial metabolisms. *Elements* **7**, 89–93.

Konhauser KO, Lalonde SV, Planavsky NJ, *et al*. (2011b) Aerobic bacterial pyrite oxidation and acid rock drainage during the Great Oxidation Event. *Nature* **478**, 369–373.

Kostka JE, Dalton DD, Skelton H, Dollhopf S, Stucki JW (2002) Growth of Fe(III)-reducing bacteria on clay minerals as the sole electron acceptor and comparison of growth yields on a variety of oxidized iron forms. *Applied and Environmental Microbiology* **68**, 6256–6262.

Krachler R, Jirsa F, Ayromlou S (2005) Factors influencing the dissolved iron input by river water to the open ocean. *Biogeosciences* **2**, 311–315.

Krachler R, Krachler RF, von der Kammer F, *et al*. (2010) Relevance of peat-draining rivers for the riverine input of dissolved iron into the ocean. *Science of the Total Environment* **408**, 2402–2408.

Krom MD, Berner RA (1980) Adsorption of phosphate in anoxic marine sediments. *Limnology and Oceanography* **25**, 797–806.

Krull-Davatzes AE, Byerly GR, Lowe DR (2010) Evidence for a low-O_2 Archean atmosphere from nickel-rich chrome spinels in 3.24 Ga impact spherules, Barberton greenstone belt, South Africa. *Earth and Planetary Science Letters* **296**, 319–328.

Kump LR, Seyfried WE Jr (2005) Hydrothermal Fe fluxes during the Precambrian: effect of low oceanic sulfate concentrations and low hydrostatic pressure on the composition of black smokers. *Earth and Planetary Science Letters* **235**, 654–662.

Langmuir D (1997) *Aqueous Environmental Geochemistry*. Prentice-Hall, Inc., Englewood Cliffs, NJ.

Lannuzel D, Schoemann V, de Long J, Chou L, Delille B, Becquevort S, Tison JL (2008) Iron study during a time series in the western Weddell pack ice. *Marine Chemistry* **108**, 85–95.

Larese-Casanova P, Haderlein SB, Kappler A (2010) Biomineralization of lepidocrocite and goethite by nitrate-reducing Fe(II)-oxidizing bacteria: effect of pH, bicarbonate, phosphate and humic acids. *Geochimica et Cosmochimica Acta* **74**, 3721–3734.

Li C, Love GD, Lyons TW, Fike DA, Sessions AL, Chu X (2010) A stratified redox model for the Ediacaran ocean. *Science* **328**, 80–83.

Liang L, McCarthy JF, Jolley LW, McNabb JA, Mehlhorn TL (1993) Iron dynamics: transformation of Fe(II)/Fe(III) during injection of natural organic matter in a sandy aquifer. *Geochimica et Cosmochimica Acta* **57**, 1987–1999.

Lilley MD, Feely RA, Trefry JH (2004) Chemical and biochemical transformations in hydrothermal plumes. In: *Seafloor Hydrothermal Systems: Physical, Chemical, Biological, and Geological Interactions* (eds Humphris SE, Zierenberg RA, Mullineaux LS, Thomson RE). American Geophysical Union Monograph 91, Washington, DC, pp. 369–391.

Lovley DR, Coates JD, Blunt-Harris EL, Phillips EJP, Woodward JC (1996) Humic substances as electron acceptors for microbial respiration. *Nature* **382**, 445–448.

Lovley DR, Holmes DE, Nevin KP (2004) Dissimilatory Fe(III) and Mn(IV) reduction. *Advances in Microbial Physiology* **49**, 219–286.

Lower SK, Hochella MF Jr, Beveridge TJ (2001) Bacterial recognition of mineral surfaces: nanoscale interactions between Shewanella and a-FeOOH. *Science* **292**, 1360–1363.

Luther GW III (1991) Pyrite synthesis via polysulfide compounds. *Geochimica et Cosmochimica Acta* **55**, 2839–2849.

Lyons TW, Severmann S (2006) A critical look at iron paleoredox proxies: new insights from modern euxinic marine basins. *Geochimica et Cosmochimica Acta* **70**, 5698–5722.

Lyons TW, Gellatly AM, McGoldrick PJ, Kah LC (2006) Proterozoic sedimentary exhalative (SEDEX) deposits and links to evolving global ocean chemistry. *Geological Society of America Memoirs* **198**, 169–184.

Lyons TW, Anbar AD, Severmann S, Scott C, Gill BC (2009a) Tracking euxinia in the ancient ocean: a multiproxy perspective and Proterozoic case study. *Annual Review of Earth and Planetary Sciences* **37**, 507–534.

Lyons TW, Reinhard CT, Scott C (2009b) Redox redux. *Geobiology* **7**, 489–494.

Lyons TW, Anbar AD, Bekker A, *et al*. (2010) New view of the old ocean: a prevalence of deep iron and marginalized sulfide from the Late Archean through the Proterozoic. *Geological Society of America Abstracts with Programs* **42**, 560.

Marsili E, Baron DB, Shikhare ID, Coursolle D, Gralnick JA, Bond DR (2008) Shewanella secretes flavins that mediate extracellular electron transfer. *Proceedings of the National Academy of Sciences* **105**, 3968–3973.

Martin JM, Fitzwater SE (1988) Iron deficiency limits phytoplankton growth in the north-east Pacific subarctic. *Nature* **331**, 341–343.

McDonough WF (2003) Compositional model for the Earth's core. In: *Treatise on Geochemistry* (eds Holland HD, Turekian KK), Vol. 2: *The Mantle and Core* (ed Carlson RW). Elsevier, Oxford, pp. 547–568.

McFadden KA, Huang J, Chu X, *et al*. (2008) Pulsed oxidation and biological evolution in the Ediacaran Doushantuo Formation. *Proceedings of the National Academy of Sciences* **105**, 3197–3202.

McLennan SM (2001) Relationships between the trace element composition of sedimentary rocks and upper continental crust. *Geochemistry, Geophysics, Geosystems* **2**, 1021, Paper number 2000GC000109.

Melezhik VA, Fallick AE, Rychanchik DV, Kuznetsov AB (2005) Palaeoproterozoic evaporites in Fennoscandia: implications for seawater sulphate, d13C excursions and the rise of atmospheric oxygen. *Terra Nova* **17**, 141–148.

Meyer KM, Kump LR (2008) Oceanic euxinia in Earth history: causes and consequences. *Annual Review of Earth and Planetary Sciences* **36**, 251–288.

Michel FM, Barrón V, Torrent J, *et al*. (2010) Ordered ferrimagnetic form of ferrihydrite reveals links among structure, composition, and magnetism. *Proceedings of the National Academy of Sciences* **107**, 2787–2792.

Millero FJ, Hawke DJ (1992) Ionic interactions of divalent metals in natural waters. *Marine Chemistry* **40**, 19–48.

Millero FJ, Yao W, Aicher J (1995) The speciation of Fe(II) and Fe(III) in natural waters. *Marine Chemistry* **50**, 21–39.

Miot J, Benzerara K, Morin M, *et al*. (2009) Iron biomineralization by neutrophilic iron-oxidizing bacteria. *Geochimica et Cosmochimica Acta* **73**, 696–711.

Morris RC (1993) Genetic modelling for banded iron-formation of the Hamersley Group, Pilbara Craton, Western Australia. *Precambrian Research* **60**, 243–286.

Muehe M, Gerhardt S, Schink B, Kappler A (2009) Ecophysiology and energetic benefit of mixotrophic Fe(II)-oxidation by nitrate-reducing bacteria. *FEMS Microbiology Ecology* **70**, 335–343.

Murakami T, Sreenivas B, Sharma SD, Sugimori H (2011) Quantification of atmospheric oxygen levels during the Paleoproterozoic using paleosol compositions and iron oxidation kinetics. *Geochimica et Cosmochimica Acta* **75**, 3982–4004.

Nealson KH (1982) Microbiological oxidation and reduction of iron. In: *Mineral Deposits and the Evolution of the Biosphere* (eds Holland HD, Schidlowski M). Springer-Verlag, New York, pp. 51–66.

Neilands JB (1989) Siderophore systems of bacteria and fungi. In: *Metal Ions and Bacteria* (ed Doyle RJ). John Wiley & Sons, New York, pp. 141–163.

Nevin K, Lovley D (2000) Lack of production of electron-shuttling compounds or solubilization of Fe(III) during reduction of insoluble Fe(III) oxide by Geobacter metallireducens. *Applied and Environmental Microbiology* **66**, 2248–2251.

Page WJ (1993) Growth conditions for the demonstration of siderophores and iron-repressible outer membrane proteins in soil bacteria, with an emphasis on free-living diazotrophs. In: *Iron Chelation in Plants and Soil Microorganisms* (eds Barton LL, Hemming BC). Academic Press, Inc., New York, pp. 75–110.

Palme H, Jones A (2003) Solar system abundances of the elements. In: *Treatise on Geochemistry* (eds Holland HD, Turekian KK), Vol. 1: *Meteorites, Comets, and Planets* (ed Davis AM). Elsevier, Oxford, UK, pp. 41–61.

Palme H, O'Neill, HSC (2003) Cosmochemical estimates of mantle composition. In: *Treatise on Geochemistry* (eds Holland HD, Turekian KK), Vol. 2: *The Mantle and Core* (ed Carlson RW). Elsevier, Oxford, UK, pp. 1–38.

Pavlov AA, Kasting JF (2002) Mass-independent fractionation of sulfur isotopes in Archean sediments: strong evidence for an anoxic Archean atmosphere. *Astrobiology* **2**, 27–41.

Perry EC, Tan FC, Morey GB (1973) Geology and stable isotope geochemistry of the Biwabik Iron Formation, northern Minnesota. *Economic Geology* **68**, 1110–1125.

Pirajno F, Hocking RM, Reddy SM, Jones AJ (2009) A review of the geology and geodynamic evolution of the Palaeoproterozoic Earaheedy Basin, Western Australia. *Earth-Science Reviews* **94**, 39–77.

Phoenix VR, Konhauser KO, Adams DG, Bottrell SH (2001) Role of biomineralization as an ultraviolet shield: implications for Archean life. *Geology* **29**, 823–826.

Planavsky N, Rouxel O, Bekker A, Shapiro R, Fralick P, Knudsen A (2009) Iron-oxidizing microbial ecosystems thrived in late Paleoproterozoic redox-stratified oceans. *Earth and Planetary Science Letters* **286**, 230–242.

Planavsky NJ, Rouxel O, Bekker A, *et al*. (2010a) The evolution of the marine phosphate reservoir. *Nature* **467**, 1088–1090.

Planavsky NJ, Bekker A, Rouxel OJ, *et al*. (2010b) Rare Earth Element and yttrium compositions of Archean and Paleoproterozoic Fe formations revisited: new perspectives on the significance and mechanisms of deposition. *Geochimica et Cosmochimica Acta* **74**, 6387–6405.

Planavsky NJ, McGoldrick P, Scott CT, *et al*. (2011) Widespread iron-rich conditions in the mid-Proterozoic ocean. *Nature* **477**, 448–451.

Posth NR, Hegler F, Konhauser KO, Kappler A (2008) Alternating Si and Fe deposition caused by temperature fluctuations in Precambrian oceans. *Nature Geoscience* **1**, 703–708.

Posth NR, Huelin S, Konhauser KO, Kappler A (2010) Size, density and mineralogy of cell-mineral aggregates formed during anoxygenic phototrophic Fe(II) oxidation. *Geochimica et Cosmochimica Acta* **74**, 3476–3493.

Poulton SW, Canfield DE (2011) Ferruginous conditions: a dominant feature of the ocean through Earth's history. *Elements* **7**, 107–112.

Poulton SW, Raiswell R (2002) The low-temperature geochemical cycle of iron: from continental fluxes to marine sediment deposition. *American Journal of Science* **302**, 774–805.

Poulton SW, Fralick PW, Canfield DE (2004) The transition to a sulphidic ocean ~1.84 billion years ago. *Nature* **431**, 173–177.

Poulton SW, Fralick PW, Canfield DE (2010) Spatial variability in oceanic redox structure 1.8 billion years ago. *Nature Geoscience* **3**, 486–490.

Radic A, Lacan F, Murray JW (2011) Iron isotopes in the seawater of the equatorial Pacific Ocean: new constraints for the oceanic iron cycle. *Earth and Planetary Science Letters* **306**, 1–10.

Raiswell R (2011) Iron transport from the continents to the open ocean: the aging-rejuvenation cycle. *Elements* **7**, 101–106.

Raiswell R, Canfield DE (1998) Sources of iron for pyrite formation in marine sediments. *American Journal of Science* **298**, 219–245.

Raiswell R, Benning LG, Tranter M, Tulaczyk S (2008) Bioavailable iron in the Southern Ocean: the significance of the iceberg conveyor belt. *Geochemical Transactions* **9**, 7.

Rakshit S, Matocha CJ, Coyne MS (2008) Nitrite reduction by siderite. *Soil Science Society of America Journal* **72**, 1070–1077.

Rashby SE, Sessions AL, Summons RE, Newman DK (2007) Biosynthesis of 2-methylbacteriohopanepolyols by an anoxygenic phototroph. *Proceedings of the National Academy of Sciences* **104**, 15099–15104.

Rasmussen B, Buick R (1999) Redox state of the Archean atmosphere: evidence from detrital heavy minerals in ca. 3250–2750 Ma sandstones from the Pilbara Craton, Australia. *Geology* **27**, 115–118.

Rasmussen B, Fletcher IR, Brocks JJ, Kilburn MR (2008) Reassessing the first appearance of eukaryotes and cyanobacteria. *Nature* **455**, 1101–1104.

Reguera G, McCarthy KD, Mehta T, Nicoll JS, Tuominen MT, Lovley DR (2005) Extracellular electron transfer via microbial nanowires. *Nature* **435**, 1098–1101.

Reinhard CT, Raiswell R, Scott C, Anbar AD, Lyons TW (2009) A Late Archean sulfidic sea stimulated by early oxidative weathering of the continents. *Science* **326**, 713–716.

Ries JB, Fike DA, Pratt LM, Lyons TW, Grotzinger JP (2009) Superheavy pyrite (d34Spyr > d34SCAS) in the terminal Proterozoic Nama Group, southern Namibia: a consequence of low seawater sulfate at the dawn of animal life. *Geology* **37**, 743–746.

Roden EE (2003) Fe(III) oxide reactivity toward biological versus chemical reduction. *Environmental Science & Technology* **37**, 1319–1324.

Roden EE, Zachara JM (1996) Microbial reduction of crystalline iron(III) oxides: influence of oxide surface area and potential for cell growth. *Environmental Science & Technology* **30**, 1618–1628.

Roden EE, Kappler A, Bauer I, *et al*. (2010) Extracellular electron transfer through microbial reduction of solid-phase humic substances. *Nature Geoscience* **3**, 417–421.

Rosing MT, Frei R (2004) U-rich Archaean sea-floor sediments from Greenland – indications of >3700 Ma oxygenic photosynthesis. *Earth and Planetary Science Letters* **217**, 237–244.

Rouxel OJ, Bekker A, Edwards KJ (2005) Iron isotope constraints on the Archean and Paleoproterozoic ocean redox state. *Science* **307**, 1088–1091.

Russell MJ, Hall AJ (1997) The emergence of life from iron monosulphide bubbles at a submarine hydrothermal redox and pH front. *Journal of the Geological Society of London* **154**, 377–402.

Rye R, Holland HD (1998) Paleosols and the evolution of atmospheric oxygen: a critical review. *American Journal of Science* **298**, 621–672.

Schädler S, Burkhardt C, Hegler F, *et al*. (2009) Formation of cell-iron-mineral aggregates by phototrophic and nitrate-reducing anaerobic Fe(II)-oxidizing bacteria. *Geomicrobiology Journal* **26**, 93–103.

Schoonen MAA, Barnes HL (1991) Reactions forming pyrite and marcasite from solution: II. Via FeS precursors below 100°C. *Geochimica et Cosmochimica Acta* **55**, 1505–1514.

Schröder S, Bekker A, Beukes NJ, Strauss H, van Niekerk HS (2008) Rise in seawater sulphate concentration associated with the Paleoproterozoic positive carbon isotope excursion: evidence from sulphate evaporites in the ~2.2–2.1 Gyr shallow-marine Lucknow Formation, South Africa. *Terra Nova* **20**, 108–117.

Scott C, Lyons TW, Bekker A, *et al*. (2008) Tracing the stepwise oxygenation of the Proterozoic ocean. *Nature* **452**, 456–459.

Scott CT, Bekker A, Reinhard CT, *et al*. (2011) Late Archean euxinic conditions before the rise of atmospheric oxygen. *Geology* **39**, 119–122.

Sekine Y, Tajika E, Tada R, *et al*. (2011) Manganese enrichment in the Gowganda Formation of the Huronian Supergroup: a highly oxidizing shallow-marine environment after the last

Huronian glaciation. *Earth and Planetary Science Letters* **307**, 201–210.

Severmann S, Lyons TW, Anbar A, McManus J, Gordon G (2008) Modern iron isotope perspective on the benthic iron shuttle and the redox evolution of ancient oceans. *Geology* **36**, 487–490.

Severmann S, McManus J, Berelson WM, Hammond DE (2010) The continental shelf benthic iron flux and its isotope composition. *Geochimica et Cosmochimica Acta* **74**, 3984–4004.

Shen Y, Canfield DE, Knoll AH (2002) Middle Proterozoic ocean chemistry: evidence from the McArthur Basin, northern Australia. *American Journal of Science* **302**, 81–109.

Shen Y, Knoll AH, Walter MR (2003) Evidence for low sulphate and anoxia in a mid-Proterozoic marine basin. *Nature* **423**, 632–635.

Shen Y, Zhang T, Hoffman PF (2008) On the coevolution of Ediacaran oceans and animals. *Proceedings of the National Academy of Sciences* **105**, 7376–7381.

Silverman MP, Lundgren DG (1959) Studies on the chemoautotrophic iron bacterium Ferrobacillus ferrooxidans II. Manometric studies. *Journal of Bacteriology* **78**, 326–331.

Singer PC, Stumm W (1970) Acidic mine drainage: the rate-determining step. *Science* **167**, 1121–1123.

Slack JF, Cannon WF (2009) Extraterrestrial demise of banded iron formations 1.85 billion years ago. *Geology* **37**, 1011–1014.

Slack JF, Grenne T, Bekker A, Rouxel OJ, Lindberg PA (2007) Suboxic deep seawater in the late Paleoproterozoic: evidence from hematitic chert and iron formation related to seafloor-hydrothermal sulfide deposits, central Arizona, USA. *Earth and Planetary Science Letters* **255**, 243–256.

Slack JF, Grenne T, Bekker A (2009) Seafloor-hydrothermal Si-Fe-Mn exhalites in the Pecos greenstone belt, New Mexico, and the redox state of ca. 1720 Ma deep seawater. *Geosphere* **5**, 302–314.

Stefánsson A (2007) Iron(III) hydrolysis and solubility at 25°C. *Environmental Science & Technology* **41**, 6117–6123.

Steinhoefel G, von Blanckenburg F, Horn I, *et al*. (2010) Deciphering formation processes of banded iron formations from the Transvaal and the Hamersley successions by combined Si and Fe isotope analysis using UV femtosecond laser ablation. *Geochimica et Cosmochimica Acta* **74**, 2677–2696.

Straub KL, Benz M, Schink B, Widdel F (1996) Anaerobic, nitrate-dependent microbial oxidation of ferrous iron. *Applied and Environmental Microbiology* **62**, 1458-1460.

Straub KL, Buchholz-Cleven BEE (1998) Enumeration and detection of anaerobic ferrous iron-oxidizing, nitrate-reducing bacteria from diverse European sediments. *Applied and Environmental Microbiology* **64**, 4846-4856.

Sugimori H, Yokoyama T, Murakami T (2009) Kinetics of biotite dissolution and Fe behavior under low O_2 conditions and their implications for Precambrian weathering. *Geochimica et Cosmochimica Acta* **73**, 3767–3781.

Summons RE, Jahnke LL, Hope JM, Logan GM (1999) 2-Methylhopanoids as biomarkers for cyanobacterial oxygenic photosynthesis. *Nature* **400**, 554–557.

Summons RE, Bradley AS, Jahnke LL, Waldbauer JR (2006) Steroids, triterpenoids and molecular oxygen. *Philosophical Transactions of the Royal Society B* **361**, 951–968.

Sverjensky DA, Lee N (2010) The Great Oxidation Event and mineral diversification. *Elements* **6**, 31–36.

Tangalos GE, Beard BL, Johnson CM, *et al*. (2010) Microbial production of isotopically light iron(II) in a modern chemically precipitated sediment and implications for isotopic variations in ancient rocks. *Geobiology* **8**, 197–208.

Taylor SR, McLennan SM (1985) *The Continental Crust: Its Composition and Evolution*. Blackwell, Malden, MA.

Teutsch N, Schmid M, Müller B, Halliday AN, Bürgmann H, Wehrli B (2009) Large iron isotope fractionation at the oxic-anoxic boundary in Lake Nyos. *Earth and Planetary Science Letters* **285**, 52–60.

Thamdrup B (2000) Bacterial manganese and iron reduction in aquatic sediments. In: *Advances in Microbial Ecology*, Vol. 16 (ed Schink B). Kluwer Academic/Plenum Publishers, New York, pp. 41–84.

Toner BM, Fakra SC, Manganini SJ, *et al*. (2009) Preservation of iron(II) by carbon-rich matrices in a hydrothermal plume. *Nature Geoscience* **2**, 197–201.

Trendall AF (2002) The significance of iron-formation in the Precambrian stratigraphic record. *International Association of Sedimentologists Special Publication* **33**, 33–66.

Turick CE, Tisa LS, Caccavo F Jr (2002) Melanin production and use as a soluble electron shuttle for Fe(III) oxide reduction and as a terminal electron acceptor by Shewanella algae BrY. *Applied and Environmental Microbiology* **68**, 2436–2444.

Urrutia MM, Roden EE, Fredrickson JK, Zachara JM (1998) Microbial and surface chemistry controls on the reduction of synthetic Fe(III) oxide minerals by the dissimilatory iron-reducing bacterium *Shewanella alga*. *Geomicrobiology* **15**, 269–291.

Vargas M, Kashefi K, Blunt-Harris EL, Lovley DR (1998) Microbiological evidence for Fe(III) reduction on early Earth. *Nature* **395**, 65–67.

Verhoeven O, Mocquet A, Vacher P, *et al*. (2009) Constraints on thermal state and composition of the Earth's lower mantle from electromagnetic impedances and seismic data. *Journal of Geophysical Research* **114**, B03302.

Von Canstein H, Ogawa J, Shimizu S, Lloyd JR (2008) Secretion of flavins by Shewanella species and their role in extracellular electron transfer. *Applied and Environmental Microbiology* **74**, 615–623.

Wächtershäuser G (1988) Before enzymes and templates: theory of surface metabolism. *Microbiological Reviews* **52**, 452–484.

Waldbauer JR, Sherman LS, Sumner DY, Summons RE (2009) Late Archean molecular fossils from the Transvaal Supergroup record the antiquity of microbial diversity and aerobiosis. *Precambrian Research* **169**, 28–47.

Walker JCG (1984) Suboxic diagenesis in banded iron formations. *Nature* **309**, 340–342.

Weber KA, Pollock J, Cole KA, O'Connor SM, Achenbach LA, Coates JD (2006) Anaerobic nitrate-dependent iron(II) bio-oxidation by a novel lithoautotrophic betaproteobacterium, strain 2002. *Applied and Environmental Microbiology* **72**, 686-694.

Welander PV, Coleman ML, Sessions AL, Summons RE, Newman DK (2010) Identification of a methylase required for 2-methylhopanoid production and implications for the interpretation of sedimentary hopanes. *Proceedings of the National Academy of Sciences* **107**, 8537–8542.

Widdel F, Schnell S, Heising S, Ehrenreich A, Assmus B, Schink B (1993) Ferrous iron oxidation by anoxygenic phototrophic bacteria. *Nature* **362**, 834–836.

Wilhelm SW, Trick CG (1994) Iron-limited growth of cyanobacteria: multiple siderophore production is a common response. *Limnology and Oceanography* **39**, 1979–1984.

Wille M, Kramers JD, Nägler TF, *et al*. (2007) Evidence for a gradual rise of oxygen between 2.6 and 2.5 Ga from Mo isotopes and Re-PGE signatures in shales. *Geochimica et Cosmochimica Acta* **71**, 2417–2435.

Wille M, Nägler TF, Lehmann B, Schröder S, Kramers JD (2008) Hydrogen sulphide release to surface waters at the Precambrian/Cambrian boundary. *Nature* **453**, 767–769.

Wilson JP, Fischer WW, Johnston DT, *et al*. (2010) Geobiology of the late Paleoproterozoic Duck Creek Formation, Western Australia. *Precambrian Research* **179**, 135–149.

Xiong J (2006) Photosynthesis: what color was its origin? *Genome Biology* **7**, 245.

Yamaguchi KE, Johnson CM, Beard BL, Ohmoto H (2005) Biogeochemical cycling of iron in the Archean-Paleoproterozoic Earth: constraints from iron isotope variations in sedimentary rocks from the Kaapvaal and Pilbara Cratons. *Chemical Geology* **218**, 135–169.

Young GM (2002) Stratigraphic and tectonic settings of Proterozoic glaciogenic rocks and banded iron-formations: relevance to the snowball Earth debate. *Journal of African Earth Sciences* **35**, 451–466.